Contract No:

This document was prepared in conjunction with work accomplished under Contract No. DE-AC09-08SR22470 with the U.S. Department of Energy (DOE) Office of Environmental Management (EM).

Disclaimer:

PRODUCT/PROCESS (P/P) MODELS FOR THE DEFENSE WASTE PROCESSING FACILITY (DWPF): MODEL RANGES AND VALIDATION RANGES FOR FUTURE PROCESSING

C.M. Jantzen

T.B. Edwards

SEPTEMBER 2015

SRNL-STI-2014-00320, Revision 0

DISCLAIMER

Printed in the United States of America

Prepared for
U.S. Department of Energy

SRNL-STI-2014-00320
Revision 0

Keywords: *DWPF, process control, viscosity, durability, liquidus, glass, reduction/oxidation (REDOX)*

Retention: *Permanent*

Product/Process Models for the Defense Waste Processing Facility (DWPF): Model Ranges and Validation Ranges for Future Processing

C.M. Jantzen
T.B. Edwards

September 2015

Prepared for the U.S. Department of Energy under contract number DE-AC09-08SR22470.

Savannah River National Laboratory™
OPERATED BY SAVANNAH RIVER NUCLEAR SOLUTIONS

REVIEWS AND APPROVALS

AUTHORS:

_____

C.M. Jantzen, Engineering Process Development Date

_____

T.B. Edwards, Engineering Process Development Date

TECHNICAL REVIEW:

_____

K.M. Fox, Hanford Mission Programs Date

APPROVAL:

_____

E.N. Hoffman, Manager
Engineering Process Development Date

_____

A.P. Fellinger, Manager Date
Environmental & Chemical Process Technology Research Programs

_____

E.J. Freed, Manager Date
DWPF Engineering

ACKNOWLEDGEMENTS

This research reviewed in this document was sponsored by the Department of Energy Environmental Management (DOE EM-20 and DOE EM-50), the Savannah River Defense Waste Processing Facility (DWPF), the Mixed Waste Focus Area (MWFA), the Tank Focus Area (TFA), and the Environmental Science and Technology Program (EMSP) in connection with work done under Contract No. DE-AC09-96SR18500 with the U.S. Department of Energy. The development of the models and the validation data was accumulated from 1988 to present under DOE Contracts No. DE-AC09-89SR18035 with E.I. DuPont deNemours & Co., Contract No. DE-AC09-96SR18500 with Westinghouse Savannah River Co. (WSRC) and Washington Group Inc. (WGI), and Contract No. DE-AC09-08SR22470 with Savannah River Nuclear Solutions (SRNS).

EXECUTIVE SUMMARY

Radioactive high level waste (HLW) at the Savannah River Site (SRS) has successfully been vitrified into borosilicate glass in the Defense Waste Processing Facility (DWPF) since 1996. Vitrification requires stringent product/process (P/P) constraints since the glass cannot be reworked once it is poured into ten foot tall by two foot diameter canisters. A unique "feed forward" statistical *process* control (SPC) was developed for this control rather than statistical *quality* control (SQC). In SPC, the feed composition to the DWPF melter is controlled *prior* to vitrification. In SQC, the glass product would be sampled *after* it is vitrified. Individual glass property-composition models form the basis for the "feed forward" SPC. The models transform constraints on the melt and glass properties into constraints on the feed composition going to the melter in order to guarantee, at the 95% confidence level, that the feed will be processable and that the durability of the resulting waste form will be acceptable to a geologic repository.

The DWPF SPC system is known as the Product Composition Control System (PCCS). The PCCS property-composition models are mechanistic and depend on the following:

- glass bonding and structure (viscosity model developed in 1991 and revised in 2005)
- thermodynamics of hydration (durability model developed in 1995)
- quasicrystalline melt species interactions including glass bonding and octahedral site preference energies (liquidus model developed in 1991 and revised in 2001)

The mechanism driving each property-composition model was represented using the minimum number of terms as possible. For example, if a set of chemical species has a similar effect on the glass bonding (i.e., all alkali species are considered to break two Si-O bonds in the viscosity model), then those species are combined into one model term. In this manner each property-composition model accounts for the observed data with a relatively simple (but necessary and sufficient) number of terms (i.e., a parsimonious representation of the glass composition) supported by known glass chemistry (i.e., a mechanistic model).

All of the PCCS models cover wider property ranges than expected in DWPF processing. The viscosity and liquidus processing models were developed over wider composition and temperature ranges than can be implemented in the DWPF melter. The PCCS mechanistic models have been assessed over composition regions outside of the regions for which they were developed in the reports associated with the development of each model. The mechanistic based models were shown to lower the risk of extrapolation (i.e., the use of a model to predict an outcome for a region beyond that over which it was developed) relative to strictly empirical based models, since empirically derived models cannot be extrapolated to compositions outside the range for which they were developed. However, variability studies to confirm the durability model predictions were recommended.

The parsimonious nature of the DWPF PCCS models excludes composition terms that were unnecessary to the implementation of the DWPF flowsheet over the last 19 years. However, validation data have been collected over the intervening years through the use of variability studies at SRNL and glass composition studies at various other institutions. In this study, the historic PCCS models are assessed against two decades of additional durability data compiled in the COMPRO™ database and additional viscosity and liquidus data that have been generated since the 2005 viscosity model and 2001 liquidus model revisions: this validation data have been evaluated in individual studies but not collectively assessed. These validation assessments of the historic PCCS models against newly generated validation data, whether it is in the DWPF compositional region or not, are discussed in the appendices of this report. The historic PCCS models are then assessed against the future composition region of interest to DWPF for the

implementation of the fully coupled flowsheet, i.e. when the Salt Waste Processing Facility (SWPF) comes on line to decontaminate salt solution.

This assessment of the PCCS models over currently available data in the SWPF composition space is a prerequisite to a follow-on and more in-depth assessment using data being generated specifically to fall with the SWPF composition space of whether the PCCS models may require additional oxide components or parameters[f] or whether the weighting factors of the current oxide components or parameters need to be adjusted to cover the composition ranges anticipated. Both the prerequisite assessment and the follow-on in depth assessment will also determine whether additional species or parameters are needed to encompass any changes in frit formulation that may be necessary, e.g. MgO and/or CaO to prevent nepheline crystallization. The specific compositional regions for future DWPF processing of SWPF streams are assessed in this document.

For the SWPF processing range, there are some data available to evaluate the viscosity model and durability model. For the liquidus model, there are no currently available data that fall in the SWPF composition region. Thus, compositional coverage is needed for the liquidus model. For the durability model, while Cs_2O concentrations up to a maximum of 1.16 wt% were tested during the development of the model in 1995, there are limited new data to assess the Cs_2O partial molar free energy effects. Also, there are limited data for TiO_2 concentrations above 2 wt%.

This prerequisite assessment indicates that a combined XO_2 term may be added to the viscosity model to incorporate TiO_2, NbO_2, ZrO_2 and ThO_2, which should all have a similar structural impact on the glass viscosity. It is also recommended that a combined XO term be added to the viscosity model to encompass CaO and MgO, which may be needed as additional frit components to minimize or prevent nepheline crystallization. Terms for TiO_2, NbO_2, ZrO_2, ThO_2, CaO and MgO are in the durability model but have not been vetted with much of the additional validation data that has been compiled over the last 19 years. Terms for TiO_2, ZrO_2, CaO, and MgO are in the liquidus model but have not been vetted with additional liquidus data. This vetting against newly derived liquidus data may require that the parameter coefficients be refitted.

Lastly, the leachate data used in the durability model may require a modification to the way in which the normalized leaching parameter is calculated for high waste loaded glasses. This is based on a requirement that has been in the ASTM C1285 (Product Consistency Test) procedure since 1994: the glass surface area (SA) must be calculated using the glass density. For higher waste loaded glasses, which are denser, a smaller SA would be calculated compared to a nominal waste loaded glass, and this has an inverse impact on the normalized release, i.e. it would be biased higher as observed for the higher waste loaded glasses examined in the durability validation data. During the 1995 durability model development the glass densities were all very similar and the impact of a varying SA on the leachate concentrations was not examined. Moreover, the bias in the high waste loaded glasses, in terms of their durability response, may be related to a ratio used in the commercial glass industry, the $SiO_2/(Na_2O+B_2O_3$ ratio). Below a critical ratio of 0.333, there is always an interconnected path of non-bridging glass forming sites that can deteriorate the durability of a glass. Both the density and the $SiO_2/(Na_2O+B_2O_3$ ratio) need to be examined relative to the leachate biases observed in the recent validation data discussed in this document. Due to the potential changes in the model terms discussed in this document, variability studies will remain essential to achieve confidence in model applicability for some time after these issues are resolved. Variability studies are also part of the DWPF's Glass Product Control Program.

[f] where a parameter is defined as a group of oxides, like the alkali oxides of Cs, Na, K, and Li, that act as a grouped or lumped parameter in a model

TABLE OF CONTENTS

LIST OF TABLES

LIST OF FIGURES

LIST OF ABBREVIATIONS

APS	Amorphous Phase Separation
ARP	Actinide Removal Process
ASME	American Society of Mechanical Engineers
ASTM	American Society for Testing and Materials
BO	Bridging Oxygen
CCC	Canister Centerline Cooling
CELS	Corning Engineering Laboratory Services
CPS	Crystalline Phase Separation
CSSX	Caustic-Side Solvent Extraction
CST	Crystalline SilicoTitanate
CVS	Chemical Variability Study
DOE	Department of Energy
DWPF	Defense Waste Processing Facility
E	Activation Energy
EA	Environmental Assessment
EM	Environmental Management
EMSP	Environmental Science and Technology Program
EPA	Environmental Protection Agency
FA	Facility Acceptance
G	Gibbs free energy
ΔG_i	Partial molar hydration free energies
ΔG_p	Preliminary hydration free energy glass dissolution estimator
HLW	High Level Waste
IDMS	Integrated DWPF Melter System
L95	Lower 95% confidence interval
LHS	Left Hand Side
MAR	Measurement Acceptable Region
MCU	Modular CSSX Unit
MST	MonoSodium Titanate
MWFA	Mixed Waste Focus Area
NBO	Non-Bridging Oxygen
NQA	Nuclear Quality Assurance
OCF/SS	Owens Corning Fiberglass/Sharp Shurtz
P/P	Product/Process
PAR	Property Acceptable Region
PCCS	Product Composition Control System
PCT	Product Consistency Test
PHA	Precipitate Hydrolysis Aqueous
PNNL	Pacific Northwest National Laboratory
QAP	Quality Assurance Program
RCRA	Resource Conservation and Recovery Act
REDOX	REDuction/OXidation
RHS	Right Hand Side
ROC	Reduction of Constraints
RMSE	Root Mean Square Error
SA	Surface Area
SB	Sludge Batch
SG	Study Glasses
SGM	Scale Glass Melter
SME	Slurry Mix Evaporator
SPC	Statistical Process Control
SQC	Statistical Quality Control
SRNL	Savannah River National Laboratory

SRNS	Savannah River Nuclear Solutions
SRS	Savannah River Site
SWPF	Salt Waste Processing Facility
TCLP	Toxic Characteristic Leaching Procedure
TFA	Tank Focus Area
THERMO	Thermodynamic Hydration Energy Reaction MOdel
TRU	Transuranic
T_L	Liquidus Temperature
U95	Upper 95% confidence interval
VFT	Vogel-Fulcher-Tammann
V_r	Viscosity ratio
WASRD	Waste Acceptance System Requirement Document
WCP	Waste Form Compliance Plan
WGI	Washington Group Inc.
WL	Waste Loading
WP	Waste Processing
WSRC	Westinghouse Savannah River Co.
Z/r	Atomic charge/Atomic radius

1.0 Introduction

Borosilicate glasses have been used in the United States and in Europe to immobilize radioactive high level waste (HLW) for ultimate geologic disposal. Vitrification has also been developed as a technology to immobilize low activity waste, low-level wastes, mixed (radioactive and hazardous) wastes, and transuranic (TRU) wastes in durable glass formulations for permanent disposal and/or long-term storage. Waste glass formulations should maximize the concentration of waste in the vitrified waste form so that waste glass volumes and the associated storage and disposal costs are reduced. Moreover, the optimization of HLW glass formulations [1,2,3], or other wastes, must simultaneously balance multiple product/process (P/P) constraints (Table 1).

Table 1. Waste Glass Product and Process Constraints

Product Constraints	Process Constraints
chemical durability	melt viscosity/resistivity
glass homogeneity	liquidus
thermal stability	waste solubility
regulatory compliance	melt temperature/corrosivity
mechanical stability	radionuclide volatility
	REDuction/Oxidation (REDOX)*

* controls foaming and thus improves melt rate and controls and metal nodule formation and thus improves melter longevity

Only the chemical durability, which includes glass homogeneity, the melt viscosity, and the liquidus from Table 1 are controlled in PCCS. Thermal and mechanical stability were measured during development of the DWPF glass flowsheet.[4] Regulatory compliance with the Toxic Characteristic Leach Test (TCLP) were bounded using 1X and 10X the Environmental Protection Agency (EPA) Resource Conservation and Recovery Act (RCRA) hazardous constituents anticipated to be in glasses made from the range of wastes found in the Savannah River Site (SRS) tank farm.[5,6] Waste solubility is handled in PCCS as limits of the individual species in wt% in the glass. Melt temperature and corrosivity were optimized during extensive pilot scale testing at the SRS before DWPF startup. The melt temperature was optimized at 1150°C to minimize radionuclide volatility, afford an adequate viscosity to the melt for convection and at the same time minimize melter materials of construction corrosion, i.e. Inconel®690 and Monofrax® K-3 refractory.[7,8,9]

Melter REDOX is controlled at an $Fe^{2+}/\Sigma Fe$ target of ~0.2 and in the range of $Fe^{2+}/\Sigma Fe$ = 0.09-0.33 [10,11,12,13,14]. The REDOX model is, however, independent of PCCS. This REDOX was chosen to minimize volatilization of radionuclides (^{99}Tc and ^{104}Ru) and hazardous species such as chromium, as well as controlling melter foaming and undesirable metal nodule precipitation. Controlling the REDOX range fixes leachable species such as Cr^{6+} and Tc^{7+} in the glass in their less leachable oxidation states of Cr^{3+} and Tc^{4+}.[15]

Most P/P properties, other than melt temperature, cannot be measured directly or in-situ in the DWPF. The waste streams are often variable and difficult to characterize. In addition the P/P constraints must be satisfied to a high degree of certainty (>95%) as the canister geometry makes rework (retrieval, reformulation, and remelting) of the HLW vitrified product difficult and costly. This requires a “systems approach” so that the P/P constraints given in Table 1 can be optimized

simultaneously [1]. The "systems approach" ensures that the final product safeguards the public, and that the production process used is safe to operate.

1.1 Statistical Process Control versus Statistical Quality Control

HLW at the Savannah River Site (SRS) has successfully been vitrified into borosilicate glass in the Defense Waste Processing Facility (DWPF) since 1996. The DWPF must measure melt/glass acceptability a priori to the melter, since no remediation of the glass composition to ensure durability and processability is possible except in the vessel (i.e., in the Slurry Mix Evaporator (SME) vessel) in which frit and waste are blended. Therefore, the acceptability decision is made on the upstream process (specifically, at the SME), rather than on the downstream *melt* or glass product. That is, it is based on "feed forward" statistical *process* control[†] rather than statistical *quality* control.[††] The DWPF SPC control system is known as the Product Composition Control System (PCCS). Individual property-composition models enable the monitoring and process control strategies embedded in the DWPF PCCS.[16] These models transform constraints on the melt and glass properties such as viscosity, liquidus, and durability into constraints on feed composition.

The feed composition is used to predict the P/P properties of a melter feed using the mechanistic P/P models that relate the P/P properties to composition [2,3]. The PCCS has been shown to be a very successful "systems approach" for the past 21 years at the DWPF as PCCS was used during cold chemical startup operations (April 1994-April 1996) and for radioactive operations (April 1996-present). The feed composition to the melter is controlled *prior* to vitrification and a confirmatory glass sample is taken only once every sludge batch to confirm the glass durability (the only parameter in PCCS which is confirmed on radioactive samples). Confirmatory glass samples have been taken since radioactive startup with a frequency ranging from 6 months to 2 years and the PCCS durability model predictions have been confirmed to produce acceptable glass. After 16 years, it was recommended that these samples no longer need to be analyzed.[17] Over the last ~19 years (April 1996-March 2015) of radioactive operation approximately 4.33 $x10^6$ gallons of HLW sludge have been vitrified at the DWPF into 1.50×10^7 pounds of borosilicate glass.

1.2 Attributes of P/P Mechanistic Modeling

The DWPF property-composition models have been under development and validation since the late 1980's. Since the 1980's, the individual property models for each feed/glass constraint have been developed over wider property ranges than the feeds that were anticipated to be fed to the DWPF. The property models that have been developed are mechanistic in nature and depend on known relationships between glass structure/bonding (viscosity)[18,19], thermodynamics of melt structures and components (durability)[20,21], and quasicrystalline melt species (liquidus) [22,23,24]. The P/P models group terms with very similar effects so that each model only contains the terms that are necessary and sufficient (parsimonious) to model the P/P property of interest.

It was shown in References 18 through 25 that the DWPF mechanistic models can be applied to composition regions outside of the regions for which they were developed. The DWPF mechanistic models allow more flexibility for process control than empirical models which are (1) restricted to the compositional region over which they were developed and (2) require glass

[†] This controls the slurry feed to the melter *prior* to vitrification.
[††] Which would adjudicate product release by sampling the glass *after* it's been made.

formulations in the center of a pre-qualified glass composition region instead of in regions where waste loading can be maximized.

1.3 PCCS Models and Validation Ranges

The modeling and validation regions for each of the PCCS models that are currently in use for DWPF processing will be reviewed in this document and include the following:

- Durability model known as the Thermodyamic Hydration Energy Model (THERMO™) developed in 1995 [20,21] and the associated validation data known also as THERMO™
- Viscosity model developed in 1991 [18] and revised in 2005 [19] and the associated validation data known as VISCOMP™
- Liquidus model developed in 1991 [2] and revised in 2001 [22,23,24] and the associated validation data known as LIQCOMP™

These historic PCCS models will then be assessed against two decades of additional durability data compiled in the COMPRO™ database [26,27] and additional viscosity and liquidus data that has been generated since the 2005 viscosity model and 2001 liquidus model revisions: this validation data has been evaluated in individual studies but not collectively assessed. These assessments of the historic PCCS models against newly generated validation data are found in Appendices B, C, and D and cover a broader range than the assessment against DWPF specific composition regions discussed in the body of this study.

The historic PCCS models are then assessed against the future composition region of interest to DWPF for the implementation of the fully coupled flowsheet, i.e. when the Salt Waste Processing Facility (SWPF) comes on line to decontaminate salt solution at much higher throughput than the current Actinide Removal Process (ARP) and Modular Caustic Side Solvent Extraction Unit (MCU). This assessment of the PCCS models over the SWPF composition space is a prerequisite to a follow-on and more in-depth assessment of whether the PCCS models may require additional oxide components or parameters[f] or whether the weighting factors of the current oxide components or parameters need to be adjusted to cover the composition ranges anticipated.[28] Both the prerequisite assessment and the follow-on in depth assessment will also determine whether additional species or parameters are needed to encompass any changes in frit formulation that may be necessary, i.e. MgO and/or CaO to prevent nepheline crystallization (see Appendix A for discussion and references [29, 30, 31]). The specific compositional regions assessed in Reference 32 will be the focus of the main body of this document.

1.4 Quality Assurance

All the model assessments presented in this study were performed in accordance with DOE/RW-0333P and a Quality Assurance Program (QAP) that meets the Quality Assurance criteria specified in DOE O. 414.1, *Quality Assurance*, 10 CFR 830, *Nuclear Safety Management*, Subpart A, "*Quality Assurance Requirements*", paragraph 830.122 and also meets the requirements of ASME Nuclear Quality Assurance (NQA)-1, *Quality Assurance Requirements for Nuclear Facility Applications.*

[f] where a parameter is defined as a group of oxides, like the alkali oxides of Cs, Na, K, and Li, that act as a grouped or lumped parameter in a model

2.0 Historical Development of DWPF Process/Product (P/P) Property-Composition Models

2.1 Modeling Constraints

For all the models and validation data, various constraints are applied. The first requires that the chemical composition of the glass, on an oxide basis, be within 100±5 weight percent (wt%).[33] The "sum of oxides" constraint minimizes the impact of analytic errors during modeling and validation.

Moreover, a given glass must be homogeneous, i.e. not phase separated by liquid-liquid amorphous phase separation (APS) due to low Al_2O_3 (≤3.00 wt%), high P_2O_5 (≥2.25 wt%), or high B_2O_3 (≥15.00 wt%) concentrations.

Likewise, glasses for modeling should not be crystallized because phase separated and/or crystallized glasses can give anomalous durability [20,21,34,35,36], viscosity [37], and liquidus [38] responses. The potential impacts of crystallization on durability, i.e. a radionuclide vector from a crystal or from accelerated grain boundaries dissolution, are shown in Equation 1.

Glasses should be homogeneous (not phase separated nor crystallized) because the glass durability can be influenced by any of the four terms given in Equation 1 below. In order to minimize or eliminate the last three terms in Equation 1, so that a model represents only the effects of glass composition on the first term in the equation below, inhomogeneous glasses and crystallized glasses are excluded from modeling. Modeling includes melt insolubles as melt insolubles do not impact glass durability [21] other than that they can act as nuclei and promote crystallization [39] that can impact glass durability as shown in Equation 1.

Equation 1

$$\sum Durability = \underbrace{durability_{(homogeneous)}}_{1st\ term} + \underbrace{durability_{(amorphous\ phase\ separation)}}_{2nd\ term} + \underbrace{durability_{(crystallization)}}_{3rd\ term} + \underbrace{durability_{(accelerated\ grain\ boundary)}}_{4th\ term}$$

The glass REDOX, expressed as the $Fe^{2+}/\Sigma Fe$ ratio, must be <0.33, which is the upper limit of processability in the DWPF melter. This is because REDOX values <0.33 have been shown not to impact glass durability[40,41,42], glass viscosity, or glass liquidus values, while higher REDOX ratios (more reducing values) can impact these properties. The ΣR_2O and Al_2O_3 constraints shown in Figure 1 were developed after the THERMO™ model was developed and these constraints are discussed in Section 3.1 and Appendix A.1.

The constraints, without the uncertainties factored into the values shown, are summarized graphically in Figure 1 and discussed in detail in Appendix A. These constraints are applied so that model accuracy is maximized and model error is minimized by ensuring complete glass analyses and no anomalous property responses.

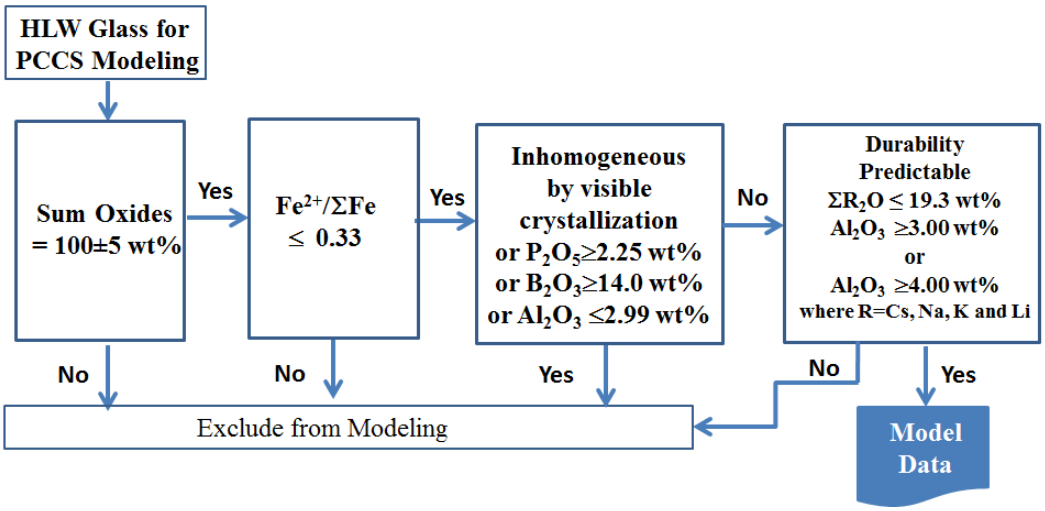

Figure 1. Graphical Representation of the Constraints Applied to the Choice of Model and Validation Data for the Durability, Viscosity, and Liquidus P/P Models. The Al_2O_3 term in the inhomogeneous by visible crystallization is 2.99 wt% to accommodate the WCP Purex glass which contains 2.99 wt% Al_2O_3.

2.2 The DWPF Durability P/P Model (1995)

The most important glass product property is the glass durability. The durability of a waste glass is the single most important variable controlling release of radionuclides and/or hazardous constituents. The intrusion of groundwater into, and passage through, a waste form burial site, in which the waste forms are emplaced, is the most likely mechanism by which constituents of concern may be removed from the waste glass and carried to the biosphere. Thus, it is important that waste glasses be stable in the presence of groundwater.

For homogeneous[f] borosilicate HLW glasses, acceptable performance is defined as an acceptably low dissolution rate, which is controlled by maintaining the glass composition within an acceptable range. The approach can be represented in terms of linking several relationships:

Equation 2

process control ↔ composition control ↔ dissolution rate control ↔ performance control ↔ acceptable performance

The linkages expressed in Equation 2 are appropriate for HLW waste glasses because the radionuclides are incorporated within the glass structure and are released congruently as the glass dissolves. In general, for any waste form it must be established that control of performance in a laboratory test predicts acceptable control of performance in a disposal system based on performance testing and modeling.

The Waste Acceptance System Requirement Document (WASRD) states that the durability and phase stability of vitrified HLW must be assessed [43], while geologic repository modeling requires the "maximum radionuclide release." These are tied together by the linking relationships shown above, i.e. that process and composition control translate into acceptable performance.

[f] no amorphous phase separation and not crystallized, i.e. the types of glasses used in the THERMO™ durability model

The "product quality constraint" on the HLW glass requires that the waste form producer demonstrate control of the waste form production by comparing production samples or process control information, separately or in combination to the Environmental Assessment (EA) benchmark glass [44,45] using the Product Consistency Test (PCT also known as ASTM C1285-14) [46] or equivalent. For acceptance, the mean concentrations of lithium, sodium, and boron in the leachate, after normalization for the concentrations in the glass, shall be 2σ less than those of the EA benchmark glass.

For borosilicate glass dissolution, the rate of release of a radionuclide from the waste form is proportional to both the dissolution rate of the waste form and the relative abundance of the radionuclide in the waste form.[47] Thus for borosilicate glass, ^{99}Tc is the radionuclide released at the fastest rate (^{137}Cs is released at a somewhat slower rate). However, extensive testing [48,49,50,51,52,53,54,55,56,57,58] demonstrated that ^{99}Tc is released congruently at the same rate as Na, Li and B for homogeneous glasses. This enables the Na, Li, and B to be measured in a glass durability test such as ASTM C1285 and be equated to the "maximum radionuclide release." The Na, Li and B are not sequestered in precipitates that participate in surface alteration reactions and are also not solubility limited.

In vitreous waste forms, the molecular structure controls dissolution (contaminant release) by establishing the distribution of ion exchange sites, hydrolysis sites, and the access of water to those sites.[35,36] Thus the DWPF durability model, THERMO™ [20,21], estimates the relative durability of silicate and borosilicate glasses based on their compositions. THERMO™ calculates the thermodynamic driving force of each glass component to hydrate based on the mechanistic role of that component during dissolution, e.g. ion exchange, matrix dissolution, accelerated matrix dissolution, surface layer formation, and/or oxidative dissolution. The overall tendency of a given glass to hydrate is expressed as a preliminary glass dissolution estimator, i.e. the change in the free energy of hydration of a glass (ΔG_p) based solely on its composition expressed as ΔG_i for the "i" different silicate and oxide components in the glass.

When the partial thermodynamic hydration free energies, ΔG_i, are weighted by the molar concentration of the silicate and oxide components present in a glass, then the overall hydration tendency of the glass can be represented by the additive contributions of the thermodynamic partial molar quantities as expressed in Equation 3

Equation 3
$$\Delta G_p = \left[\sum \left(\Delta G_i \bullet f_i\right)\right]_{T,P}$$

where ΔG_p is the preliminary free energy (G) glass dissolution estimator. The ΔG_p is based on equations that mechanistically represent glass dissolution as a process of ion exchange, matrix dissolution, and surface layer formation. The ΔG_i are the partial molar hydration free energies of the components i, and f_i are the amounts of each species expressed in dimensionless molar fractions at constant temperature and pressure.

The partial molar free energies in THERMO™ are for the species listed in Table 2 along with the compositional range used during modeling. The bolded radionuclides ranges given in Table 2 are for the DWPF pour stream samples from 1996 to present since each pour stream sample that has been leached using ASTM C1285 has been found to be acceptable. These DWPF pour stream samples are not given in ComPro™ database [26,27] used for validation and discussed in Section 3.3. Therefore, the pour stream data from References 17,59,60 are included in Table 2 for completeness.

Since 1995 when THERMO™ was developed, partial molar free energies have been developed for HfO_2 and NpO_2.[61] In addition, a partial molar free energy was developed for Nb_2O_5.[62] While these partial free energies have been developed and are included in Table 2, they have not been assessed against the existing glass validation data for high in HfO_2, NpO_2, or Nb_2O_5 as yet.

Note that Ag° and Au° are not oxides at the DWPF REDOX range and are not included in Table 2. They are metallic and/or melt insoluble phases that do not have partial molar free energies associated with them in THERMO™.

Free energies, e.g., ΔG_p, are used rather than enthalpies because chemical durability is a chemical process and the reaction progress is related to the free energy rather than the enthalpy of the overall reaction. The more negative the ΔG_p the more readily the reaction will occur. The more positive the ΔG_p the less readily the reaction will occur.

The ΔG_p is correlated to the response of a 7 day ASTM C1285 (PCT). For homogeneous glasses, the following equations are incorporated in PCCS:

Equation 4	$\log10[NCB(g/L)]$	$= -1.9014 - 0.1812\ \Delta Gp$	$R^2 = 0.77$
Equation 5	$\log10[NCLi(g/L)]$	$= -1.5459 - 0.1468\ \Delta Gp$	$R^2 = 0.75$
Equation 6	$\log10[NCNa(g/L)]$	$= -1.8012 - 0.1710\ \Delta Gp$	$R^2 = 0.80$

where ΔG_p is in kcal/100g glass and NC_i is in g/L.

Since variability studies have been conducted for each of DWPF's sludge batches, which have included fabrication of new glasses and PCT measurements as part of such studies, a great deal of additional durability data has been compiled during the time of DWPF's processing. These results have been periodically compiled in the ComPro™ database [26,27].

Table 2. Species Included in THERMO™ or Subsequently Developed

Oxide Species	THERMO™ "Model Data" Oxide Range	Ref.	Oxide Species	THERMO™ "Model Data" Oxide Range	Ref.
Al_2O_3	1.36‡-13.90	[20,21]	**NpO_2**	8.21E-04-3.08E-03	[61]
AmO_{2*}	7.58E-05-4.95E-04	[20,21]	Na_2O	6.42-16.80	[20,21]
As_2O_3		[20,21]	Nd_2O_3	0.00-5.96	[20,21]
B_2O_3	6.10-13.30	[20,21]	NiO	0.00-2.97	[20,21]
BaO	0.00-0.66	[20,21]	P_2O_5	0.00-0.65	[20,21]
CaO	0.38-2.23	[20,21]	PbO	0.00-0.25	[20,21]
CdO		[20,21]	**PuO_2**	4.01E-03-1.65E-02	[20,21]
Ce_2O_3*	0.00-1.44	[20,21]	Rb_2O		[20,21]
CoO		[20,21]	RuO_2*	0.014-0.049ξ	[20,21]
Cr_2O_3	0.00-0.55	[20,21]	Sb_2O_3*		[20,21]
Cs_2O	0.00-1.16	[20,21]	SeO_2*		[20,21]
Cu_2O*	0.00-0.30	[20,21]	SiO_2	39.80-59.80	[20,21]
CuO*	0.00-0.33	[20,21]	SnO_{2*}		[20,21]
FeO*	0.00-8.81	[20,21]	SrO	0.00-0.45	[20,21]
Fe_2O_3*	0.00-14.30	[20,21]	**TcO_2***	5.54E-05-6.24E-04	[20,21]
HfO_2*	Validation	[61]	TeO_2		[20,21]
K_2O	0.00-5.73	[20,21]	**ThO_2**	0.68-1.00	[20,21]
La_2O_3	0.00-0.42	[20,21]	TiO_2	0.00-3.21	[20,21]
Li_2O	2.59-5.16	[20,21]	**U_3O_8***	0-3.51	[20,21]
MgO	0.00-3.24	[20,21]	Y_2O_3	Validation	[20,21]
MnO*	0.00-3.36	[20,21]	ZnO	0.00-1.46	[20,21]
MoO_3*	0.00-1.67	[20,21]	ZrO_2	0.00-1.80	[20,21]
Nb_2O_5	Validation	[62]			

*Note the species are predicted at the REDOX range over which DWPF processes.[20,21]

‡During development of THERMO™ it was determined that a minimum of 3 wt% Al_2O_3 was necessary in high Fe_2O_3 containing and high Na_2O containing glasses to avoid phase separation [63]. This is consistent with the known miscibility gap in the Al_2O_3-Fe_2O_3-Na_2O-SiO_2 quaternary system that defines the crystallization of basalt [63].

ξ From the Waste Form Compliance Plan (WCP) glass ranges. [64]

2.3 The DWPF Viscosity and Resistivity Models

The viscosity of a waste glass melt as a function of temperature is one of the most important variables affecting the melt rate[τ] and pourability of the glass. The viscosity determines the rate of melting of the raw feed, the rate of glass bubble release (foaming and fining), the rate of homogenization, the adequacy of heat transfer, the devitrification rate, and thus, the quality (in terms of glass homogeneity) of the final glass product. If the viscosity is too low, excessive convection currents can occur, increasing corrosion/erosion of the melter materials (refractories and electrodes) and making control of the waste glass melter more difficult. The lowest glass viscosities set for the DWPF waste glass melter are, therefore, conservatively set at ~20 poise at

τ Melt rate is also related to melt pool resistivity, which is highly correlated to melt pool viscosity: melt rate is also related to the REDOX of the melt pool as an oxidizing melt pool can cause O_2 foaming from manganese oxide reduction and the foam can form an insulating layer on the melt pool and inhibit heat transfer from the lid heaters.

T_{melt}. Waste glasses are usually poured continuously into steel canisters for ultimate storage. Glasses with viscosities above 500 poise do not readily pour. Moreover, too high a viscosity can reduce glass quality by causing voids in the final glass. A conservative maximum viscosity of 110 poise at T_{melt}, was, therefore, established for DWPF production.[65]

The approach taken in the development of the viscosity and resistivity process models [2,18,19] was based on glass structural considerations, expressed as a calculated non-bridging oxygen (NBO) term. This NBO parameter represents the amount of structural depolymerization in the glass (Equation 7). Oxide species were expressed in mole fraction and related to the viscosity-temperature dependence of the Fulcher equation [18,19], also known as the Vogel-Fulcher-Tammann (VFT)[‡] equation. The VFT relates the viscosity (η) of a glass to temperature (Equation 8) for Newtonian fluids. Therefore, non-Newtonian fluids, such as crystallized glasses [66] are not included in the viscosity model or validation data. Phase separated glasses are also not included in the viscosity model or validation model as they give anomalous viscosity vs. temperature plots. [37]

Equation 7 $$NBO \equiv \frac{2\,(Na_2O + K_2O + Cs_2O + Li_2O + Fe_2O_3 - Al_2O_3) + B_2O_3}{SiO_2}$$

Equation 8 $$\log_{10}\eta = A + \frac{B}{T - T_o}$$

In Equation 8, η is viscosity (poise or d•Pa[*]), T is temperature in °C, and A, B, and T_o are fitted constants. It is well documented that the overall fit of the Fulcher equation is excellent for glasses but that it also overestimates viscosity at lower temperatures in the range of viscosities $>10^{10}$ Pa.s [67]. In addition, viscosities less than 1 Pa.s (10 poise) are not modeled as ASTM C965 [68] indicates that the measurement is not accurate in this low viscosity range.

Calculation of the NBO term from molar composition was combined with quantitative statistical analyses of response surfaces to express glass viscosity and resistivity as a function of melt temperature and glass composition. The DWPF glass viscosity model was originally developed in 1991 [2,18] based on "as batched" glass compositions and the coefficients were revised in 2005 based on "as-measured" glass compositions.[19] The 2005 version of the DWPF viscosity model is given by

Equation 9 $$\log\eta(poise) = -0.519571 + \left(\frac{4453.87}{T(^oC)}\right) - (1.690326 * NBO).$$

‡ Fulcher derived this expression to model viscosity of inorganic glasses in 1925. In 1921, Vogel (Phys. Zeit., 22, 645-646) derived a similar expression for the viscosity of water, mercury, and oils and Tammann and Hesse generated a similar equation for organic liquids in 1926 (Z. Anorg. Allg. Chem. 156, 245-257). So all three are credited with the derivation of the mathematical expression and it is often referred to as the VFT equation.

* The unit of viscosity is the dyne second per square centimeter, which is called the poise. The SI unit for viscosity is the Newton second per square meter, or pascal second; one of these units equals 10 poise.

with an adjusted R^2= 0.966, and a root mean square error (RMSE) of 0.0832. Equation 9 is based on 175 viscosity-temperature points.

The DWPF viscosity model assumes that a pure SiO_2 glass is fully polymerized; i.e. there are no NBO and 4 bridging oxygen (BO) bonds. Addition of other species known as network modifiers depolymerizes the glass while network formers polymerize the glass. This approach was a simplification of an NBO term developed by White and Minser [69] to describe the structural features observed in Raman spectroscopy data of complex natural glasses (obsidians and tektites), which had no B_2O_3 and almost all FeO instead of Fe_2O_3. Equation 9 is also consistent with the usage of a viscosity ratio (V_r) to model the viscosity of slags [70]. The V_r is defined as the sum of the Z/r (atomic charge/atomic radius) of the network formers times the atomic % of the network formers divided by the sum of the Z/r of the network modifiers times the atomic % of the network modifiers.

In the DWPF viscosity model, it is assumed that each mole of alkali oxide added creates two non-bridging oxygen bonds by forming metasilicate (Na_2SiO_3) structural units; thus depolymerizing the glass. While the exact number of non-bridging oxygen atoms depends on the molar ratio of all of the species in a waste glass to SiO_2, most DWPF glasses have a O^{2-}/ Si^{4+} ratio of 2.6 to 3.3 which implies that disilicate and metasilicate structural units predominate for the alkali species in the waste glasses. Calculation of the O^{2-}/ Si^{4+} ratio for DWPF glasses included contributions from Na, K, Li, and Cs alkali species and a Si^{4+} concentration that was depleted by the amount associated with B_2O_3 structural units.

The DWPF viscosity model further assumes that each mole of Al_2O_3 creates two bridging oxygen bonds (polymerizes the glass structure) by creating tetrahedral alumina groups that bond as $NaAlO_2$ structural groups. In Al_2O_3 and/or SiO_2 deficient glasses, Fe_2O_3 can take on a tetrahedral coordination and polymerize a glass by forming $NaFeO_2$ structural groups. However, if sufficient Al_2O_3 and SiO_2 are present in a glass such as DWPF waste glasses that typically contain >3 wt% Al_2O_3 and >40 wt% SiO_2, then Fe_2O_3 is octahedral and creates two non-bridging oxygen bonds, i.e., it depolymerizes the glass matrix as assumed in the DWPF viscosity model (Equation 9). This is consistent with the work of Mysen [71] who demonstrated that high iron magmas (iron silicate glasses) that contained levels of 10 wt% Fe_2O_3 decreased the melt viscosity. He concluded that $NaFeO_2$ structural groups were not incorporated into the silicate network to the same degree as $NaAlO_2$ structural groups [71]. Therefore, Fe_2O_3 is considered a network modifier and depolymerizer in the DWPF viscosity model.

Lastly, the DWPF viscosity model assumes that each mole of B_2O_3 creates one non-bridging oxygen bond. This is based on data by Smets and Krol [72], and Konijnendijk [73] who demonstrated that for sodium silicate glasses with low B_2O_3 content the B_2O_3 enters the glass network as BO_4^- tetrahedral. At higher B_2O_3 concentrations, these tetrahedra are converted into planar BO_3^- groups. Tetrahedral BO_4^- contributes no NBO while planar BO_3^- groups contribute one non-bridging oxygen atom [74].

In 1991, the viscosity model was developed on as batched compositions [2,18] and revised [19] based on analyses of the same non-radioactive glasses and frits (220 viscosity-temperature measurements). During the 2005 revision, the model was validated [19] on an additional 200 glasses (radioactive and non-radioactive and 1004 viscosity-temperature pairs). Uranium was shown to have no impact on glass viscosity, and ThO_2 at <1 wt% had no impact on glass viscosity. The viscosity model was developed over composition and temperature regions (873-1491°C), well outside of the regions over which it can be applied in DWPF. It is applied in PCCS at the

DWPF melt temperature of 1150°C.

Equation 9 was implemented in PCCS at the DWPF melt temperature of 1150°C. However, the equation represents a three dimensional plane in composition (NBO), viscosity, and temperature space as shown in Figure 2. Therefore, the viscosity model could easily be applied at a variety of glass temperatures in a variety of different melter designs. The viscosity model covers temperatures from 873-1491°C but was validated to as low as 808°C. The model covers glasses from 10.2 poise to 122 poise but was validated up to 11,000 poise (see Appendix C). The composition covered by the 2005 DWPF viscosity model is given in Table 3.

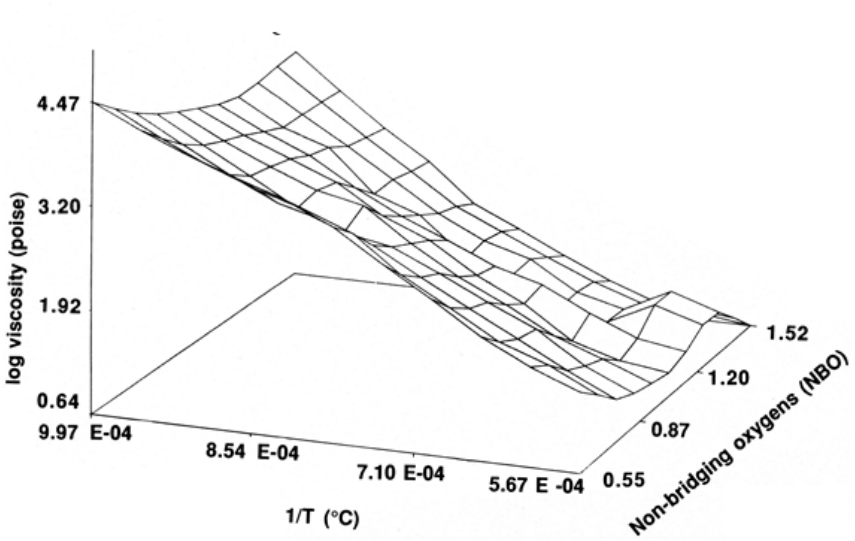

Figure 2. DWPF viscosity model showing the relationship between composition (NBO), viscosity and temperature.

Radioactive glasses were not included in the development of the 1991 DWPF viscosity model because the commercial glass laboratories that were performing the measurements could not handle radioactive glasses. The SRNL developed radioactive viscosity measurement capability in 1998. The 1991 viscosity model was re-examined in 2005 [19] to determine whether radioactive components were needed in the model and to determine the impact of having used the as batched instead of as measured glass compositions. The following was concluded:

- the 1991 DWPF PCCS viscosity model was found to be biased due to six as-batched glass compositions that were in error and two glasses that were determined to be phase separated: phase separated glasses can give anomalous viscosity response [37]

- the magnitude of the bias in the 1991 DWPF viscosity model based on as-batched glass compositions over the 7-1,000 poise range relative to the non-radioactive as-measured glasses was the same as the bias observed between the as-batched model and radioactive glasses

- the coefficients of the 1991 DWPF viscosity model were revised in 2005 using the as-measured glass compositions and eliminating the inhomogeneous glass responses and this corrected the 1991 model bias

- once the bias in the 1991 DWPF viscosity model was corrected, it was shown that a U^{+6} term was not needed and a Th^{+4} term was not needed as long as the Th^{+4} concentrations in the glass were ≤ 1wt%

- a Th^{+4} term will be necessary for DWPF glasses containing Th^{+4} >1 wt%.

An electrical resistivity model [2] was developed for the DWPF using the same NBO term given in Equation 7. However, it is not used in the DWPF because control of the viscosity in turn controls the resistivity in the operating range. The resistivity model ranges are the same as the viscosity model ranges in terms of composition. Since the DWPF does not implement the resistivity model, it has not been validated as the viscosity model has been validated.

The electrical resistivity of a waste glass melt as a function of temperature is the single most important variable affecting the establishment of Joule heating for electrically heated melters. The electrical resistivity controls the rate of melting after the establishment of Joule heating. At low temperatures, glasses are good insulators, while at high temperatures they conduct electric current relatively well. The current is transferred by ion migration: the mobility of the modifying ions is much higher than that of network formers at all temperatures. The concentration of alkali ions contributes the most to the electrical conductivity. During passage of direct current though a glass melt, the alkali ions migrate to the cathode while the glass close to the anode is enriched with SiO_2 and the resistivity locally increases. These polarization effects are eliminated by the use of alternating current as used in Joule heated melters. However, the chemical composition of a melt has a significant effect on the electrical properties [75] and the melt rate at the melt temperature.

The same melt NBO term (Equation 7) was used for glass resistivity as was used for glass viscosity, and a relationship derived between the resistivity, the inverse of the melt temperature, and the NBO based on 52 data points.[76] In 2005, the resistivity model was updated from the 1991 version with the "as-measured" compositions as well, and the unpublished refit to the data is given below.

Equation 10
$$\log \varphi(\Omega cm) = -0.42 + \left(\frac{2652.15}{T(^{o}C)}\right) - (1.5015 * NBO)$$

with an adjusted $R^2 = 0.969$ and a RMSE of 0.0938.

Table 3**. Composition, Temperature, and Viscosity Range of DWPF Viscosity Model.**

Parameter	Viscosity and Resistivity " Model Data" (33 glasses; 175 viscosity-temperature pairs)
	2005 MODEL DATA
Temperature (°C)	873-1491
Viscosity (poise)	10.2-1,122.02
$Fe^{+2}/\Sigma Fe$	0.00-0.47
Al_2O_3(wt%)	0.00-13.90
B_2O_3(wt%)	6.41-12.20
BaO(wt%)	0.00-0.20
CaO(wt%)	0.00-1.47
Cr_2O_3(wt%)	0.00-0.09
Cs_2O(wt%)	0.00-0.15
CuO(wt%)	0.00-0.33
Cu_2O(wt%)	0.00-0.30
FeO(wt%)	0.00-7.14
Fe_2O_3(wt%)	0.00-14.20
K_2O(wt%)	0.00-5.73
La_2O_3(wt%)	0.00-0.36
Li_2O(wt%)	2.59-6.96
MgO(wt%)	0.49-2.92
MnO(wt%)	0.00-3.26
Na_2O(wt%)	5.80-15.80
Nb_2O_5 (wt%)	0.00
NiO(wt%)	0.00-2.97
P_2O_5 (wt%)	0.00
SiO_2(wt%)	45.60-77.04
SrO(wt%)	0.00-0.07
ThO_2 (wt%)	0.00
TiO_2(wt%)	0.00-1.78
U_3O_8 (wt%)	0.00
ZnO(wt%)	0.00
ZrO_2(wt%)	0.00-0.99

2.4 The DWPF Liquidus Temperature Model

The DWPF liquidus temperature model prevents melt pool volume crystallization during operation. Volume crystallization needs to be avoided because it can involve almost simultaneous nucleation of the entire melt pool as volume crystallization can occur very rapidly. A liquidus limit for the DWPF was set at 1050°C (100°C lower than the nominal DWPF melt temperature) and the liquidus limit allows for no melt crystallization.[77]

Furthermore, once spinel crystals are formed (the most ubiquitous liquidus phase occurring in US defense HLW), these crystals are refractory and cannot easily or quickly be re-dissolved into an 1150°C melt pool because $NiFe_2O_4$ crystals melt at 1660°C [78] and the kinetics of dissolution at lower temperatures like 1150°C are too slow. The presence of crystals may cause the melt viscosity and resistivity to increase [79,80], which may cause difficulty in discharging glass from the melter as well as difficulty in melting via Joule heating. Once a significant

amount of volume crystallization has occurred and the resulting crystalline material has settled to the melter floor, melting may be inhibited and the pour spout may become partially or completely blocked making pouring difficult.

The original DWPF liquidus model was developed on only 22 data points.[2] The liquidus model was revised between 1997 and 2001 [22] as additional data became available. A "spinel only" liquidus model was developed assuming that spinel was the solute and nepheline and the remaining glass constituents were the solvent. However, a nepheline liquidus can be generated with more data assuming that nepheline is the solute and spinel and the remaining glass are the solvent [23,24].

The crystal-melt equilibria were modeled based on quasicrystalline concepts [23,24]. A pseudobinary phase diagram between a ferrite spinel (an incongruent melt product of transition metal iron rich acmite) and nepheline was defined. The pseudobinary lies within the Al_2O_3-Fe_2O_3-Na_2O-SiO_2 quaternary system that defines the crystallization of basalt glass melts (note that the basalt glass system is used as an analogue for waste glass durability, liquidus, and the prevention of phase separation). The liquidus model developed based on these concepts has been used to prevent unwanted crystallization in the DWPF HLW melter for the past fourteen years, while allowing waste loadings of 25-28 wt% to be raised to 36-40 wt% loadings. The liquidus model and the pseudobinary were shown [23,24] to be consistent with all of the thermal stability data generated on DWPF HLW glasses.

The liquidus model takes on the form of quasicrystalline groups expressed as oxides for the exchange reactions of the type given between the melt species (Left Hand Side, LHS) and the primary crystalline phases (Right Hand Side, RHS):

Equation 11 for normal[ξ] spinels:

$$2^{[4\text{-}6]}Ni_{0.5}{}^{[4]}AlO_2 + 2(Na,Li)^{[4]}CrO_2 + 2(K,Na)^{[4]}AlO_2 + (K,Na)_2SiO_3 + 5SiO_2$$
$$\text{melt} \qquad \text{melt} \qquad \text{melt} \qquad \text{melt} \qquad \text{melt}$$
$$\updownarrow$$
$$^{[4]}Ni^{[6]}Cr_2O_4 + 4(K,Na)^{[4]}AlSiO_4 + (Na,Li)_2Si_2O_5$$
$$\text{normal spinel} \qquad \text{nepheline} \qquad \text{disilicate}$$

Equation 12 for inverse[ξ] spinels:

$$2^{[4\text{-}6]}Ni_{0.5}{}^{[4]}AlO_2 + 2(Na,Li)^{[4]}FeO_2 + 2(K,Na)^{[4]}AlO_2 + (K,Na)_2SiO_3 + 5SiO_2$$
$$\text{melt} \qquad \text{melt} \qquad \text{melt} \qquad \text{melt} \qquad \text{melt}$$
$$\updownarrow$$

[ξ] The spinel liquidus phase that crystallizes from HLW waste glass melts is nominally $NiFe_2O_4$, an inverse $BABO_4$ spinel structure, where all the divalent elements ($^{[6]}B=Mg^{2+}$,Zn^{2+}, Fe^{2+}, Ni^{2+}) are in octahedral coordination and half of the Fe^{3+} are in octahedral coordination ($^{[6]}B$) in the B site while the remaining Fe^{3+} are tetrahedrally coordinated in the $^{[4]}A$ lattice site. Small amounts of Cr^{3+} and Al^{3+} substitution, and occasionally substitution of Ti^{4+}or Ti^{3+}, can occur in these inverse spinels. However, the remaining aluminate and chromite spinels and $MnFe_2O_4$ spinels have a "normal" spinel structure in which all of the 13 species prefer the octrahedral B sites and the Mn^{2+} occupies the $^{[4]}A$ tetrahedral lattice site. This is because the crystallographic preference of any ion for the spinel octahedral site has been found to diminish in the following order: $Cr^{3+} > Ni^{2+} > Ti^{3+} > Fe^{2+} > Fe^{3+} > Mn^{2+}$

$$^{[6]}Ni^{[4]}Fe^{[6]}FeO_4 + 4(K,Na)^{[4]}AlSiO_4 + (Na,Li)_2Si_2O_5$$
inverse spinel nepheline disilicate

The availability of cations to the various melt phase complexes or precursors can be accounted for by defining the following molar site distributions:

Pyroxene-like Complex or Precursor:[†]

$$\Sigma_{MT} \equiv \phi_{T,SiO_2} z_{SiO_2} + \phi_{T,Al_2O_3} z_{Al_2O_3} + \phi_{T,Fe_2O_3} z_{Fe_2O_3}$$

$$\Sigma_{M1} \equiv \phi_{M1,Al_2O_3} z_{Al_2O_3} + \phi_{M1,Fe_2O_3} z_{Fe_2O_3} + \phi_{M1,TiO_2} z_{TiO_2} + \phi_{M1,Cr_2O_3} z_{Cr_2O_3} + \phi_{M1,ZrO_2} z_{ZrO_2} + \phi_{M1,NiO} z_{NiO} + \phi_{M1,MgO} z_{MgO} + \phi_{M1,MnO} z_{MnO}$$

$$\Sigma_{M2} \equiv \phi_{M2,NiO} z_{NiO} + \phi_{M2,MgO} z_{MgO} + \phi_{M2,MnO} z_{MnO} + \phi_{M2,CaO} z_{CaO} + \phi_{M2,K_2O} z_{K_2O} + \phi_{M2,Li_2O} z_{Li_2O} + \phi_{M2,Na_2O} z_{Na_2O}$$

Nepheline-like Complex or Precursor:

$$\Sigma_{T1} \equiv \phi_{T1,SiO_2} z_{SiO_2} + \phi_{T1,Al_2O_3} z_{Al_2O_3} + \phi_{T1,Fe_2O_3} z_{Fe_2O_3} + \phi_{T1,TiO_2} z_{TiO_2}$$

$$\Sigma_{N1} \equiv \phi_{N1,K_2O} z_{K_2O} + \phi_{N1,Li_2O} z_{Li_2O} + \phi_{N1,Na_2O} z_{Na_2O}$$

where $\phi_{i,j}$ is the fraction of the moles of j associated with the i^{th} site and z_j represents the total moles of j per 100 grams of glass. The manner in which the fractions are defined is discussed below.

Thus, the appropriate mole fractions to use to represent the liquid phase activities for the components comprising the proposed melt phase complexes or precursors are:[†]

$$M_2 = \left[(M2)_2O_{(l)}\right] \equiv \frac{\Sigma_{M2}}{\Sigma}, \quad M_1 = \left[(M1)_2O_{3(l)}\right] \equiv \frac{\Sigma_{M1}}{\Sigma}, \text{ and } \quad M_T = \left[(MT)O_{2(l)}\right] \equiv \frac{\Sigma_{MT}}{\Sigma}$$

where

$$\Sigma \equiv \Sigma_{M2} + \Sigma_{M1} + \Sigma_{MT} + \Sigma_{T1} + \Sigma_{N1}$$

because only the pyroxene-nepheline pseudobinary is of concern. The pyroxene melt phase precursor liquid phase activity can then be approximated by:

Equation 13
$$a\left(P_{(l)}\right) \approx K_P \left(M_2\right)^a \left(M_1\right)^b \left(M_T\right)^c$$

and then, upon substitution, becomes:

Equation 14
$$-R \ln\left\{K_P \left(M_2\right)^a \left(M_1\right)^b \left(M_T\right)^c\right\} \approx \Delta\overline{H}_{fus,P}\left(T_P^*\right)\left(\frac{1}{T_L} - \frac{1}{T_P^*}\right).$$

[†] A term representing the ZnO concentration must be added to ΣM_2 when the liquidus temperatures of glasses containing significant concentrations of this oxide are to be predicted.

[†] This appears consistent with the concept of site fractions (i.e., the number of atoms in a particular structural site divided by the total number of sites of that type available) that is normally applied to the chemistry of imperfect crystals. For more information, please refer to: F.A. Kroger, **The Chemistry of Imperfect Crystals**, North-Holland Pub. Co., Amsterdam, The Netherlands, 1039 pp. (1964).

that provides a relationship between melt concentrations and the liquidus temperature, T_L. Rearranging the above relationship provides a way to estimate the (reciprocal) liquidus temperature as a function of the molar melt constituent concentrations:

Equation 15

$$\left(\frac{1}{T_L}\right) \approx -\frac{R}{\Delta\overline{H}_{fus,P}\left(T_P^*\right)}\ln\left\{M_2{}^{a}M_1{}^{b}M_T{}^{c}\right\}+\left\{\left(\frac{1}{T_P^*}\right)-\frac{R\ln\left(K_P\right)}{\Delta\overline{H}_{fus,P}\left(T_P^*\right)}\right\}.$$

Equation 15 provides a parsimonious basis for predicting liquidus temperature for waste glasses assuming the presence of a pyroxene intermediate that then melts incongruently to spinel.

By fitting the form of Equation 15 to data, Equation 16 is generated.

Equation 16

$$\frac{1}{T_L(K)_{spinel}} = -0.000260\ln(M_2)-0.000566\ln(M_1)-0.000153\ln(M_T)-0.00144$$
$$= \ln\left\{(M_2)^{-0.000260}(M_1)^{-0.000566}(M_T)^{-0.000153}\right\}-0.00144$$

where

$$\Sigma_{MT} \equiv \phi_{T,SiO_2}z_{SiO_2}+\phi_{T,Al_2O_3}z_{Al_2O_3}+\phi_{T,Fe_2O_3}z_{Fe_2O_3}$$
$$\Sigma_{M1} \equiv \phi_{M1,Al_2O_3}z_{Al_2O_3}+\phi_{M1,Fe_2O_3}z_{Fe_2O_3}+\phi_{M1,TiO_2}z_{TiO_2}+\phi_{M1,Cr_2O_3}z_{Cr_2O_3}+\phi_{M1,ZrO_2}z_{ZrO_2}$$
$$+\phi_{M1,NiO}z_{NiO}+\phi_{M1,MgO}z_{MgO}+\phi_{M1,MnO}z_{MnO}$$
$$\Sigma_{M2} \equiv \phi_{M2,NiO}z_{NiO}+\phi_{M2,MgO}z_{MgO}+\phi_{M2,MnO}z_{MnO}+\phi_{M2,CaO}z_{CaO}$$
$$+\phi_{M2,K_2O}z_{K_2O}+\phi_{M2,Li_2O}z_{Li_2O}+\phi_{M2,Na_2O}z_{Na_2O}$$
$$\Sigma_{T1} \equiv \phi_{T1,SiO_2}z_{SiO_2}+\phi_{T1,Al_2O_3}z_{Al_2O_3}+\phi_{T1,Fe_2O_3}z_{Fe_2O_3}+\phi_{T1,TiO_2}z_{TiO_2}$$
$$\Sigma_{N1} \equiv \phi_{N1,K_2O}z_{K_2O}+\phi_{N1,Li_2O}z_{Li_2O}+\phi_{N1,Na_2O}z_{Na_2O}$$

and

$$M_2 \equiv \frac{\Sigma_{M2}}{\Sigma}, M_1 \equiv \frac{\Sigma_{M1}}{\Sigma}, M_T \equiv \frac{\Sigma_{MT}}{\Sigma}, \text{and } \Sigma \equiv \Sigma_{M2}+\Sigma_{M1}+\Sigma_{MT}+\Sigma_{T1}+\Sigma_{N1}.$$

and R^2 = 0.89. The details of the modeling are given elsewhere [22] and the range of compositions over which the liquidus model was developed are given in Table 4.

Table 4. Composition Range of DWPF Liquidus Model.

Oxide Species (wt%)	Liquidus "Model Data" (105 glasses; 55 measured at SRNL and 50 PNNL)[22,23,24]
Temperature	799-1304
Al_2O_3	0.99-14.16
B_2O_3	4.89-12.65
BaO	NM*
CaO	0.31-2.01
Cr_2O_3	0.00-0.30
Cs_2O	NM
FeO	0.02-6.90
Fe_2O_3	3.43-16.98
$(\Sigma Fe)_2O_3$	3.45-17.60
K_2O	0.00-3.89
Li_2O	2.49-6.16
MgO	0.47-2.65
MnO	0.74-3.25
Na_2O	5.99-14.90
Nd_2O_3	NM*
NiO	0.04-3.05
P_2O_5	NM*
SiO_2	41.80-58.23
SO_4	NM*
TiO_2	0.00-1.85
U_3O_8	0.00-5.14
ZrO_2	0.00-0.97

*NM= not measured, PNNL = Pacific Northwest National Laboratory

2.5 Control Chart of DWPF Processing 1996-2014 Using Historical PCCS Models

A summary table of the calculated properties that the DWPF Melter #1 and Melter #2 have seen over the last 21 years of processing (including cold chemical campaigns) is provided in Appendix E). The property summaries are presented in Figure 3 as control charts to demonstrate how the historical PCCS models have kept the DWPF vitrification process in control using SPC for the last 21 years. It should be noted that the last three points on the liquidus control chart in Figure 3 are not plotted. This is because during the non-radioactive DWPF qualification campaigns (the far right side of each part of Figure 3) it was determined that the high Cr_2O_3 in the analyzed glass samples was coming from the steel grinders being used to prepare the samples.[81] An abnormally high Cr_2O_3 content in a glass analysis gives an erroneously high liquidus temperature using the current DWPF liquidus model as Cr_2O_3 content is highly correlated to the liquidus temperature. After DWPF qualification campaigns only non-steel containing grinders were used to analyze glass.

The PCCS glass properties have been calculated from canisters that were sectioned during cold campaigns and calculated for radioactive operations based on DWPF pour stream sample analyses. The measured compositions of the glasses used in the control chart are also given in Appendix E.

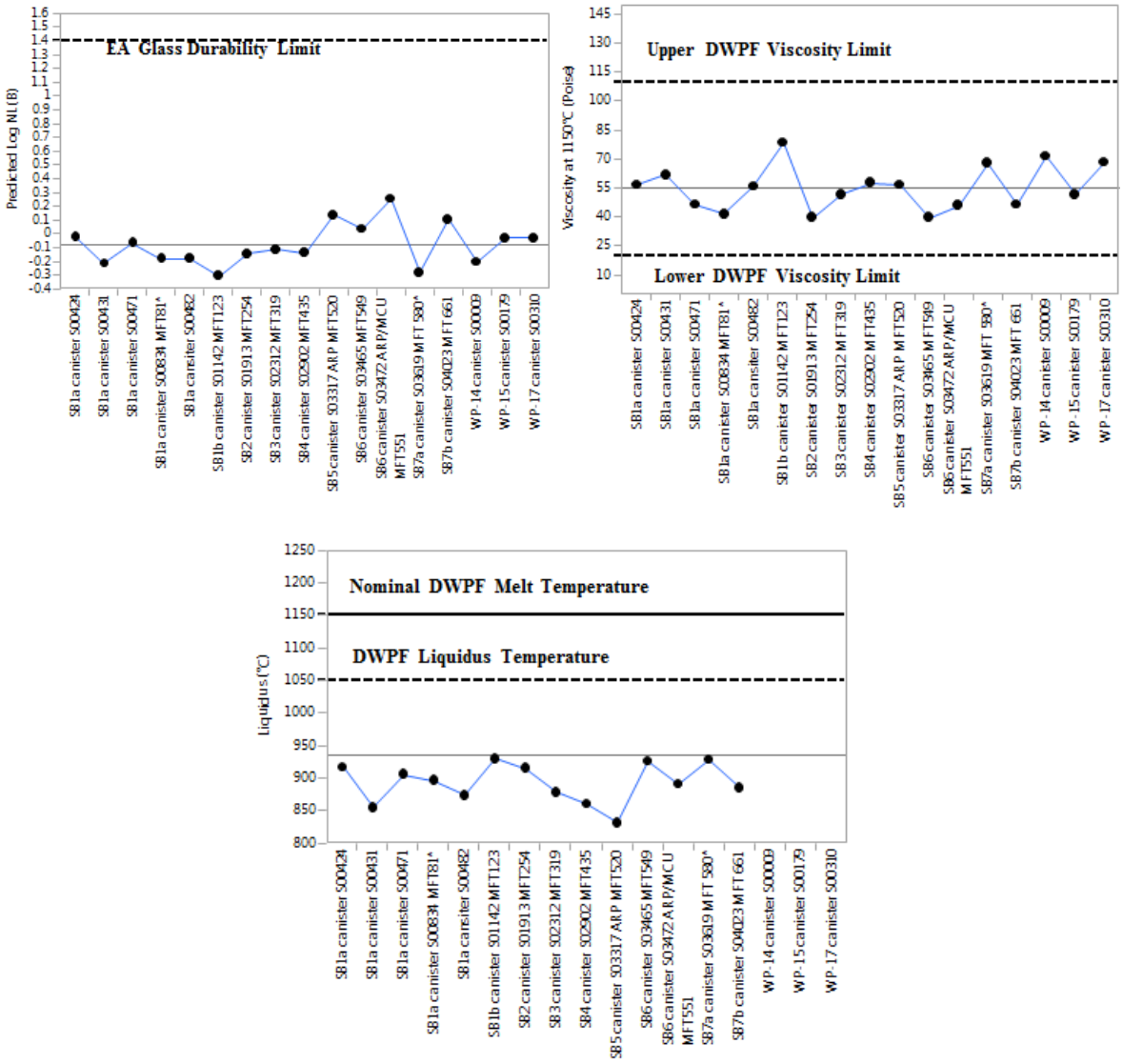

Figure 3. Control Chart of DWPF PCCS Properties 1994-present

3.0 Assessment of DWPF PCCS Models with Predicted Future Processing Compositions

3.1 Defining Future DWPF Processing Ranges

With the initiation of the ARP and MCU at SRS in 2008, there was a need to revisit the DWPF homogeneity constraint shown in Figure 1 and discussed in Appendix A for coupled operations. This constraint was specifically addressed through the variability study for Sludge Batch 5 (SB5). However, additional benefit would be gained if the homogeneity constraint could be replaced by the Al_2O_3 and sum of alkali constraint for future fully coupled operations composition projections as was done for sludge only processing in DWPF.

Raszewski and Edwards [82] conducted a reduction of constraints (ROC) study for coupled operations. The region covered by this study is provided in Table 5. The "Others" component in this table includes: BaO, CdO, Ce_2O_3, La_2O_3, PbO, SO_4, ZnO, and ZrO_2. PCTs were conducted and evaluated for the glasses tested as part of this study, which led to the replacement of the homogeneity constraint, in its entirety, by the following criteria

(1) use the alumina constraint as currently implemented in PCCS ($Al_2O_3 \geq 3$ wt%) and add a sum of alkali constraint with an upper limit of 19.3 wt% ($\sum R_2O < 19.3$ wt%), or

(2) adjust the lower limit on the Al_2O_3 constraint to 4 wt% ($Al_2O_3 \geq 4$ wt%),

for coupled operations with TiO_2 levels up to 2 wt% in glass [82]. Furthermore, Table 5 also defines the compositional region of interest for coupled operations at DWPF with TiO_2 levels up to 2 wt%.

Table 5. Oxide Intervals for Reduction of Constraints Study for Coupled Operations with ARP and MCU

Oxide	Minimum (wt%)	Maximum (wt%)
Al_2O_3	3.25	18
B_2O_3	4.5	14
CaO	0	4
Cr_2O_3	0	0.2
Fe_2O_3	5	21
Li_2O	4	7
MgO	0	1.5
MnO	0.3	5.5
Na_2O	10	18
NiO	0	2.5
SiO_2	30	55
TiO_2	0.5	2.0
U_3O_8	0	9.5
Others	0	2.0

The information in Table 5 was used to support an effort to define any potential gaps in the compositional range of the current models when compared to the compositional region projected

for the SWPF flowsheet. In addition to addressing this issue for the models discussed above, the gap analysis study currently underway [28,32, 83] is to extend the reduction of constraints coverage to the glass composition region anticipated for the DWPF and SWPF coupled flowsheet. From reference 83, the compositional region of interest is defined by the oxides and wt% intervals given in Table 6. In this table, the shaded oxide rows define the "others" component for this compositional region.

Thus, one may look to the glass regions of Table 5 and Table 6 to define the region of interest for assessing the applicability of the current property-composition models.

Table 6. Oxide Intervals for SWPF Gap Analysis Study

Oxide	Minimum (wt%)	Maximum (wt%)
Al_2O_3	3.5	13
B_2O_3	4.5	10
BaO	0	0.25
CaO	0.2	2
Ce_2O_3	0	0.2
CoO	0	0.1
Cr_2O_3	0	0.2
Cs_2O	0.3	1
CuO	0	0.1
Fe_2O_3	5	16
K_2O	0	0.2
La_2O_3	0	0.1
Li_2O	1	7
MgO	0	2
MnO	0.2	4
Na_2O	8	18
NiO	0	2
PbO	0	0.25
SO_4	0	0.3
SiO_2	40	55
ThO_2	0	1
TiO_2	2	6
U_3O_8	0	6
ZnO	0	0.2
ZrO_2	0	0.25

All of the assessments of the property-composition models presented in this report were conducted using JMP Pro Version 11.2.1 [84]. To facilitate these assessments, the glass compositions were screened for their applicability for the regions defined by Table 5 and Table 6. Figure 4 provides an example of the formula developed in JMP to conduct this screening. Each compositional variable (i.e., each of the oxides) shown in this figure is in weight percent concentrations and the inequality expression(s) for each variable must be met for the composition to be within the DWPF region of interest.

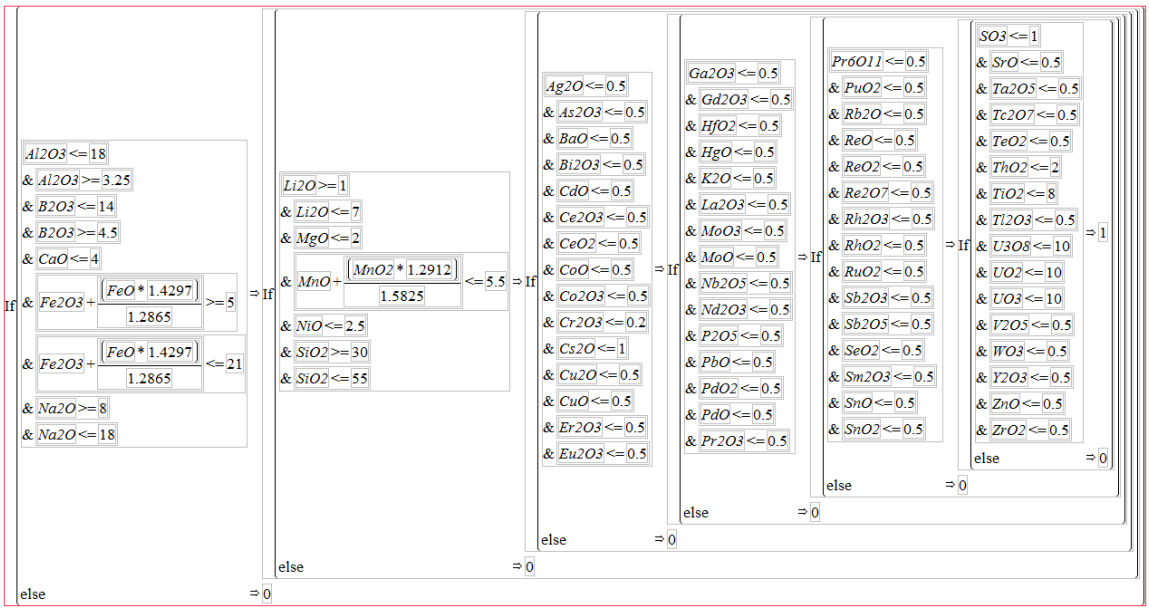

Figure 4. JMP Formula Used to Select DWPF-Like Compositions for this Study.

3.2 Approach to Defining Applicable Composition Region for DWPF Processing

Three JMP databases served as the sources of information for this review of the property-composition models. The ComPro™ database, Revision 2 (see [26] and [27]), was used to assess the validity of the THERMO™ glass durability models are to the compositional regions defined by Table 5 and Table 6.

The VISCOMP™ database that was used to generate the DWPF viscosity model [18], augmented by the validation data given in Reference 19 was used to investigate the validation range for the viscosity model. Additional validation data have been generated since Reference 19 was published and these are referenced in Appendix C. The data in Reference 19 and the additional data called out in Table 10 were used to assess how valid the DWPF viscosity model is over the compositional regions defined by Table 5 and Table 6.

The LIQCOMP™ database that was used to generate the DWPF liquidus model, augmented by the validation data in Reference 22 and the SCM-2 run [23,24], was used to assess the validity of the DWPF liquidus model over the compositional regions defined by Table 5 and Table 6. Other liquidus validation data given in Appendix D could not be used due to a variety of measurement errors and/or lack of identification of the liquidus phase(s) since the DWPF liquidus model is a spinel only liquidus model.

3.3 Assessment of PCCS Durability Model and Validation Ranges in DWPF Future Processing Range

Since the development of the THERMO™ model [21] was completed, SRNL has compiled a database of glass compositional and PCT response information that covers a broad glass compositional region. The data from numerous glass studies across the DOE complex including the data used in the development of the THERMO™ model, have been incorporated into this database, which is called ComPro™. Revision 2 of this database (see [26] and [27]) was used to facilitate the investigation into the performance (i.e., the ability to provide reliable predictions) of the THERMO™ models over the compositional region defined by Table 5 and Table 6 as represented in Figure 4.

The data from ComPro™ were screened for applicability for this study. The data from ComPro™ were screened for applicability for this study. Specifically, only data from studies of sufficient quality assurance (i.e., those studies that meet the requirements of RW-0333P and designated as "Model" in ComPro™) were considered in this investigation. In addition, the other constraints associated with durability (see the SME acceptability reference [85]) were imposed on the entries in ComPro™: these were the constraints for Al_2O_3/sum of alkali and nepheline. Only ComPro™ entries satisfying all of these constraints at least to the Property Acceptability Region (PAR) criteria [85] were considered as part of the current evaluation.

Two additional levels of screening were conducted on the entries in ComPro™ beyond those described above. The formula, given in Figure 4, was used to screen the entries in ComPro™ against the compositional regions defined by Table 5 and Table 6. Only the ComPro™ entries that satisfied the constraints imposed by that JMP formula were included in this investigationThe heat treatment information in ComPro™ was used to conduct a final screening process. Two groups of glasses were considered for this evaluation: quenched glasses and center-line canister cooled (ccc) glasses.[ε] The combined set of quenched and ccc results yielded 2628 of the original 13479 ComPro™ entries for this study. A closer look only at the quenched glasses (1464 results) is also provided in the discussion that follows.

The evaluation utilized the PCT results for boron, lithium, and sodium for each entry in this subset of ComPro™. A routine "predictability" criterion was used to label each entry: if the measured elemental PCT response (expressed as a common logarithm of the normalized release in g/L) fell within the 95% confidence interval for an individual prediction conducted using JMP for the THERMO™ model fit for that element, then the entry for that element was labeled as "predictable." Otherwise, the ComPro™ entry was labeled as "unpredictable" for the durability model for that element. The results (i.e., the percent of the ComPro entries that were predictable) for the durability models of the three elements may be summarized as follows:

Table 7. Predictability of Durability Responses by Element

% Predictable	Boron	Lithium	Sodium
quenched & ccc	89.3%	89.4%	93.0%
quenched only	89.6%	89.2%	92.7%

The validity of the durability models for process control for a specific DWPF sludge batch is confirmed by the supporting glass variability study for that sludge batch. Then, too, additional insight into the performance of the models can be gained by a closer look at these ComPro™ results.

Table 8 provides a summary of the boron evaluation for the subset of ComPro™ entries that passed the screening process. Included in this table is a row showing the number of entries: 280 entries that were not predictable and 2348 entries that were predictable for the combined set of ccc and quenched glasses. Thus, 280 of 2628 or 10.7% of the entries were not predictable. Considering only the quenched glasses, 152 of 1464 or 10.4% of the entries were not predictable. As an example of the compositional information, consider the shaded row in Table 8 for Al_2O_3. It shows that the model failed to adequately predict the durability of glasses that contained Al_2O_3 in concentrations as low as 3.25 wt% to as high as 16.40 wt%, but adequately predicting the

[ε] This can be done as the spinel primary phase does not lead to additional terms in Equation 1 from the crystallization.

durability of other glasses with Al_2O_3 concentrations in the same interval. Thus, there was no discernable connection between Al_2O_3 concentrations alone and predictable versus unpredictable boron PCT responses. This was true not only for Al_2O_3 but also for the other individual oxides, and it was also true not only for the set of quenched results but also for the ccc and quenched combined results. The last two columns of Table 8 provide the compositional region evaluated for the durability models based upon this subset of ComPro™ data. For this region, the concentrations of combinations of oxides, expressed as the properties, more than the concentration of individual oxides appear to lead to a small set of unpredictable situations. In other words the "predictable" and "unpredictable" oxide ranges overlap; a closer look at these situations is provided below.

Table 8. Boron PCT Predictability of Glasses in the Selected Subsets of ComPro™ Data

	ComPro Subset ccc and quenched					ComPro Subset quenched only				**Compositional Region Evaluated for Durability Models**	
	NOT Predictable		Predictable			NOT Predictable		Predictable			
	280		2348			152		1312			
Oxide	min	max	min	max		min	max	min	max	min	max
Al_2O_3	3.25	16.40	3.25	16.40		3.25	15.64	3.25	16.40	3.25	16.40
B_2O_3	4.50	14.00	4.50	14.00		4.50	14.00	4.50	14.00	4.50	14.00
BaO	0.00	0.09	0.00	0.10		0.00	0.09	0.00	0.10	0.00	0.10
CaO	0.00	4.00	0.00	4.00		0.00	4.00	0.00	4.00	0.00	4.00
CdO	0.00	0.32	0.00	0.32		0.00	0.32	0.00	0.30	0.00	0.32
Ce_2O_3	0.00	0.37	0.00	0.39		0.00	0.37	0.00	0.39	0.00	0.39
CoO	0.00	0.01	0.00	0.01		0.00	0.00	0.00	0.01	0.00	0.01
Cr_2O_3	0.00	0.20	0.00	0.20		0.00	0.20	0.00	0.20	0.00	0.20
Cs_2O	0.00	0.00	0.00	0.00		0.00	0.00	0.00	0.00	0.00	0.00
CuO	0.00	0.14	0.00	0.15		0.00	0.14	0.00	0.15	0.00	0.15
Fe_2O_3	5.00	20.86	5.00	19.95		5.00	20.86	5.00	19.95	5.00	20.86
K_2O	0.00	0.49	0.00	0.49		0.00	0.48	0.00	0.49	0.00	0.49
La_2O_3	0.00	0.11	0.00	0.38		0.00	0.11	0.00	0.38	0.00	0.38
Li_2O	2.80	7.00	2.44	7.00		2.87	7.00	2.44	7.00	2.44	7.00
MgO	0.00	1.94	0.00	2.00		0.00	1.80	0.00	2.00	0.00	2.00
MnO	0.30	5.50	0.23	5.50		0.30	5.50	0.23	5.50	0.23	5.50
MoO_3	0.00	0.00	0.00	0.03		0.00	0.00	0.00	0.03	0.00	0.03
Na_2O	8.87	18.00	8.65	18.00		8.87	18.00	8.65	18.00	8.65	18.00
Nb_2O_5	0.00	0.08	0.00	0.47		0.00	0.08	0.00	0.47	0.00	0.47
Nd_2O_3	0.00	0.00	0.00	0.06		0.00	0.00	0.00	0.06	0.00	0.06
NiO	0.00	2.50	0.00	2.50		0.00	2.50	0.00	2.50	0.00	2.50
P_2O_5	0.00	0.49	0.00	0.49		0.00	0.32	0.00	0.49	0.00	0.49
PbO	0.00	0.23	0.00	0.25		0.00	0.22	0.00	0.25	0.00	0.25
RuO_2	0.00	0.03	0.00	0.07		0.00	0.00	0.00	0.07	0.00	0.07
SiO_2	32.45	54.97	32.45	55.00		32.45	54.97	35.99	55.00	32.45	55.00
SnO_2	0.00	0.01	0.00	0.07		0.00	0.00	0.00	0.07	0.00	0.07
SO_3	0.00	0.68	0.00	1.00		0.00	0.68	0.00	1.00	0.00	1.00
SrO	0.00	0.09	0.00	0.01		0.00	0.09	0.00	0.01	0.00	0.09
ThO_2	0.00	0.86	0.00	1.26		0.00	0.86	0.00	1.26	0.00	1.26
TiO_2	0.00	6.28	0.00	8.00		0.00	6.28	0.00	8.00	0.00	8.00
U_3O_8	0.00	8.85	0.00	9.50		0.00	8.85	0.00	9.50	0.00	9.50
ZnO	0.00	0.15	0.00	0.17		0.00	0.14	0.00	0.17	0.00	0.17
ZrO_2	0.00	0.41	0.00	0.50		0.00	0.41	0.00	0.50	0.00	0.50

Figure 5 provides a graphical representation of the boron PCT responses for the subset of 2491 ccc and quenched entries of ComPro™. The x-axis of this plot shows the ΔG_p value for the entry, i.e., the preliminary free energy of hydration determined from the glass composition, while the y-axis shows the common logarithm of the boron PCT response in g/L. Note that the results for the EA glass, which are shown for reference, have a ΔG_p value on the x-axis of −15.518 and an

average y-axis value of log(16.7) ≈ 1.22. The other points of the graph have been labeled to indicate their heat treatment: "○" – for ccc and "+" – for quenched. Three lines are shown on the plot. The predicted boron response for the ΔG_p value on the x-axis is the middle line with the bounding lines forming a 95% confidence limit for an individual prediction. Points that fall above the upper confidence limit or below the lower confidence limit are not well predicted by the model. The "unpredictable" entries fall into three categories:

1. the points corresponding to the more positive values of ΔG_p (say, for values more positive than −10.0,
2. the points falling below the lower confidence limit, and
3. the points with values of ΔG_p less than −10.0 that fall above the upper confidence limit.

PCT outcomes in the first category were seen during the development of the THERMO™ models [20] and occasionally during other glass studies such as the ROC study by Raszewski and Edwards [82] and the Sludge Batch 7b (SB7b) variability study [86]. Few of these results are seen as being a major issue since the PCT responses on the y-axis are usually far from that for the EA standard glass. The second category of points demonstrates that some glass compositions are more durable than the model indicates. That is, the model (conservatively) over predicts the PCT response for these glasses. Since they are conservative, these results, which have been seen in the variability studies for Sludge Batch 7a (SB7a) [87], SB7b [86], and Sludge Batch 8 (SB8) [88], are not perceived as being a major issue. The third category, those glasses with more negative ΔG_p values that are under predicted, is seen as the major concern. Figure 6 provides a closer look at these three categories of unpredictable results, and this plot was used to isolate and identify those ComPro™ entries falling into the third category. For reference, values for the EA glass have been added to this plot.

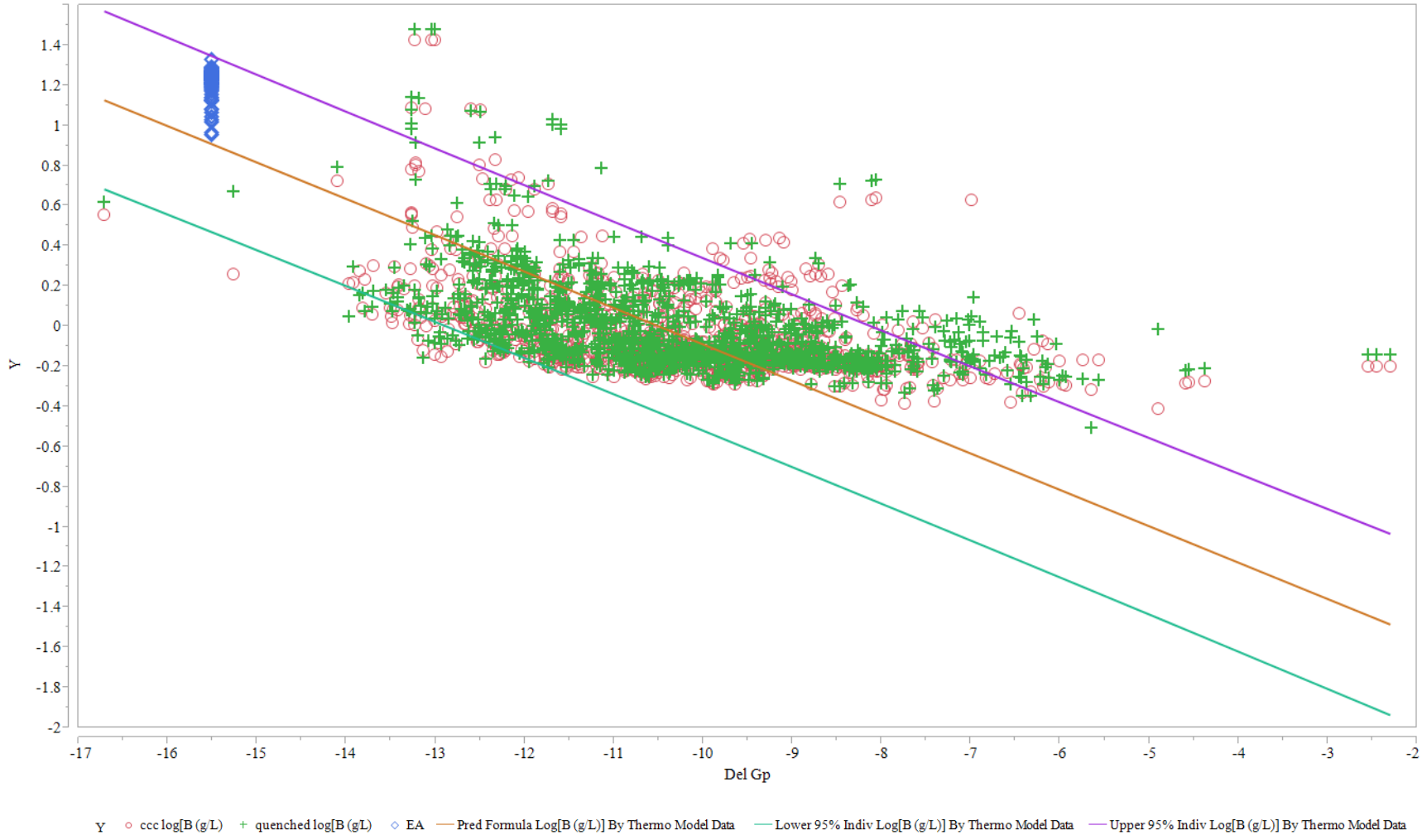

Figure 5. Predictability of Boron PCT for Subset of ComPro™ Entries

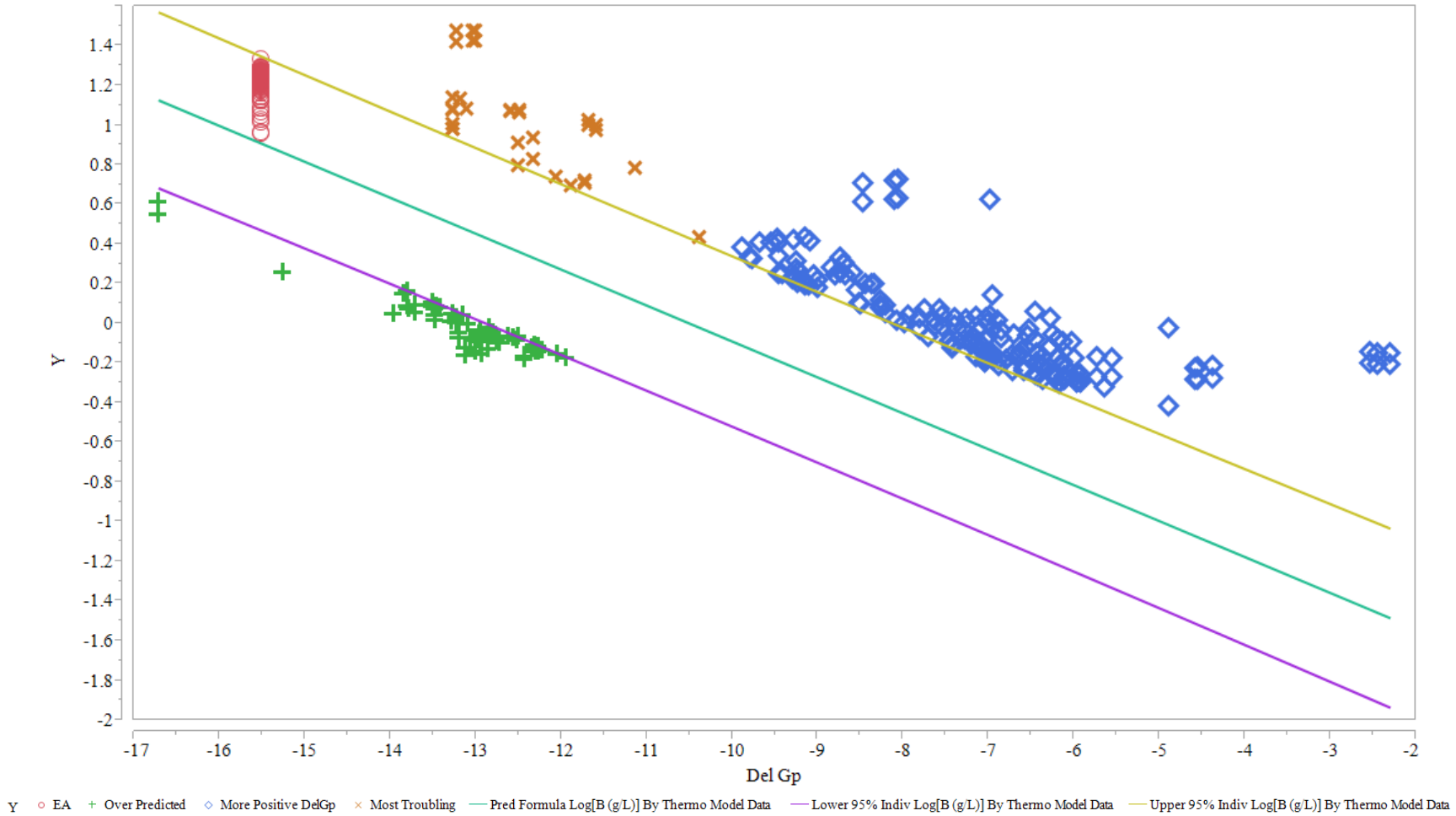

Figure 6. The Unpredictable Boron PCT Responses for the Subset of ComPro™ Entries

Table 9 provides a listing of select entries from category 2 (i.e., the less durable results) and all of the category 3 ComPro™ entries: in all 39 entries of the original 2628 entries, or about 1.5%. A review of the Table 9 ComPro™ entries shows that each of these glasses was part of a study covering a broad glass compositional region such as ROC or higher waste-loaded glass (FY09EM21) studies [see reference 118]. For studies that targeted a broad glass composition region, operational feasibility of the compositions selected for study is always a challenge. That is, the goal in designing such a study is to balance the coverage of the compositional region with the feasibility of the selected compositions to be representative of the actual operational flowsheet for the facility. As one attempts to meet this goal, there are occasions where a selected glass contains components in a combination that may yield measured properties that are difficult to predict. This may be the case for some of the entries of Table 9.

The bias indicated for the higher waste-loaded glasses in the "unpredictable" categories 1 and 3 above may be an impact of the higher density of the glasses, i.e. higher Fe_2O_3, higher MnO, higher NiO and higher TiO_2, at higher waste loadings. The 2014 revision of the PCT procedure [46] requires that the density of a glass be used to calculate the surface area (SA) term in the denominator of the normalized release formula for any element released from a glass. The formalism is SA =(6*mass)/ density*diameter of particle (m^2). If the mass and particle size are constants, then a denser glass gives a smaller SA. Since the SA appears in the denominator of the normalized release calculation, the normalized release would be biased higher. This parameter needs to be investigated in light of the high waste loaded glasses being biased high in Figure 6.

Alternatively, the bias indicated for the higher waste-loaded glasses in the "unpredictable" categories 1 and 3 above may be an impact of the lower concentration of glass formers, i.e. SiO_2, B_2O_3, and Al_2O_3, in a glass caused by an increase in the waste loading species which are not glass formers. Indeed, it is generally accepted that the rate-limiting step in silica-water reactions is breakage of the structural Si-O and Al-O bonds. Thus for a pure silica glass where there is <67 mol% silica in the presence of glass modifier cations like alkali and alkaline earth oxides,i.e. in a $CaO\text{-}Na_2O\text{-}SiO_2$ glass, there is always an interconnected path of nonbridging oxygen (=Si-O-) sites that allows exchange of species between a leachate solution and the glass. At >67 mol% silica, these sites are isolated from each other by the silica network (+Si⁻O⁻Si+ groups) in the glass that suppress the movement of ions involved in leaching. In borosilicate glasses, there is a region of poor durability that is a sliding scale of the ratio of $SiO_2/(Na_2O+B_2O_3)$. Below a critical ratio of 0.333 for this ratio, there is always an interconnected path of nonbridging glass forming sites that can impact the durability of a glass.[89] This parameter also needs to be investigated in light of the high waste loaded glasses being biased high in Figure 6.

Table 9. Category 3 and Select Category 2 Unpredictable ComPro™ Entries

(Category 2 Entries are Shaded)

Report Number	Glass ID	Heat Treatment	Compositional View	Reference	PCT B (g/L)	Del Gp
SRNL-STI-2009-00778	FY09EM21-08	ccc	Measured	FY-09 Enhanced DOE HLW Melter Throughput Studies at SRNL	4.273	-8.109
SRNL-STI-2009-00778	FY09EM21-08	ccc	Measured bc	FY-09 Enhanced DOE HLW Melter Throughput Studies at SRNL	4.335	-8.060
SRNL-STI-2009-00778	FY09EM21-08	ccc	Targeted	FY-09 Enhanced DOE HLW Melter Throughput Studies at SRNL	4.149	-8.470
SRNL-STI-2009-00778	FY09EM21-08	quenched	Measured	FY-09 Enhanced DOE HLW Melter Throughput Studies at SRNL	5.284	-8.109
SRNL-STI-2009-00778	FY09EM21-08	quenched	Measured bc	FY-09 Enhanced DOE HLW Melter Throughput Studies at SRNL	5.362	-8.060
SRNL-STI-2009-00778	FY09EM21-08	quenched	Targeted	FY-09 Enhanced DOE HLW Melter Throughput Studies at SRNL	5.131	-8.470
SRNL-STI-2009-00778	FY09EM21-14	ccc	Targeted	FY-09 Enhanced DOE HLW Melter Throughput Studies at SRNL	4.247	-6.987
SRNL-STI-2009-00778	EM-22	quenched	Measured bc	FY-09 Enhanced DOE HLW Melter Throughput Studies at SRNL	2.754	-10.387
SRNL-STI-2009-00465	ROC-16	quenched	measured bc	Reduction of Constraints for Coupled Operation	4.985	-11.893
SRNL-STI-2009-00465	ROC-16	ccc	measured	Reduction of Constraints for Coupled Operation	5.109	-11.731
SRNL-STI-2009-00465	ROC-16	quenched	measured	Reduction of Constraints for Coupled Operation	5.285	-11.731
SRNS-STI-2008-00099 Revision 0	NP2-03	ccc	Target	Refinement of the Nepheline Discriminator: Phase II Study	5.503	-12.073
SRNL-STI-2009-00778	FY09EM21-04	quenched	Targeted	FY-09 Enhanced DOE HLW Melter Throughput Studies at SRNL	6.150	-11.144
SRNL-STI-2009-00465	ROC-20	ccc	measured bc	Reduction of Constraints for Coupled Operation	6.346	-12.511
SRNL-STI-2009-00465	ROC-20	ccc	measured	Reduction of Constraints for Coupled Operation	6.742	-12.328
SRNL-STI-2009-00465	ROC-20	quenched	measured bc	Reduction of Constraints for Coupled Operation	8.240	-12.511
SRNL-STI-2009-00465	ROC-20	quenched	measured	Reduction of Constraints for Coupled Operation	8.755	-12.328
SRNL-STI-2009-00465	ROC-09	quenched	measured bc	Reduction of Constraints for Coupled Operation	9.546	-11.591
SRNL-STI-2009-00465	ROC-09RM	quenched	targeted	Reduction of Constraints for Coupled Operation	9.622	-13.273
SRNL-STI-2009-00465	ROC-09	quenched	targeted	Reduction of Constraints for Coupled Operation	9.679	-13.273
SRNL-STI-2009-00465	ROC-09M	quenched	measured bc	Reduction of Constraints for Coupled Operation	10.031	-11.591
SRNL-STI-2009-00465	ROC-09	quenched	measured	Reduction of Constraints for Coupled Operation	10.142	-11.688
SRNL-STI-2009-00465	ROC-09M	quenched	targeted	Reduction of Constraints for Coupled Operation	10.170	-13.273
SRNL-STI-2009-00465	ROC-09M	quenched	measured	Reduction of Constraints for Coupled Operation	10.657	-11.688
SRNL-STI-2009-00778	FY09EM21-02	quenched	Measured	FY-09 Enhanced DOE HLW Melter Throughput Studies at SRNL	11.720	-12.492
SRNL-STI-2009-00778	FY09EM21-02	quenched	Measured bc	FY-09 Enhanced DOE HLW Melter Throughput Studies at SRNL	11.816	-12.605
SRNL-STI-2009-00778	FY09EM21-02	ccc	Measured	FY-09 Enhanced DOE HLW Melter Throughput Studies at SRNL	11.930	-12.492
SRNL-STI-2009-00778	FY09EM21-02	quenched	Targeted	FY-09 Enhanced DOE HLW Melter Throughput Studies at SRNL	11.993	-13.272
SRNL-STI-2009-00778	FY09EM21-02	ccc	Measured bc	FY-09 Enhanced DOE HLW Melter Throughput Studies at SRNL	12.028	-12.605
SRNL-STI-2009-00778	FY09EM21-03	ccc	Targeted	FY-09 Enhanced DOE HLW Melter Throughput Studies at SRNL	12.164	-13.118
SRNL-STI-2009-00778	FY09EM21-02	ccc	Targeted	FY-09 Enhanced DOE HLW Melter Throughput Studies at SRNL	12.208	-13.272
SRNL-STI-2009-00778	FY09EM21-07	quenched	Targeted	FY-09 Enhanced DOE HLW Melter Throughput Studies at SRNL	13.643	-13.182
SRNL-STI-2009-00778	FY09EM21-07	quenched	Measured	FY-09 Enhanced DOE HLW Melter Throughput Studies at SRNL	13.866	-13.274
SRNL-STI-2009-00778	FY09EM21-21	ccc	Targeted	FY-09 Enhanced DOE HLW Melter Throughput Studies at SRNL	26.542	-13.226
SRNL-STI-2009-00778	FY09EM21-21	ccc	Measured bc	FY-09 Enhanced DOE HLW Melter Throughput Studies at SRNL	26.713	-13.007
SRNL-STI-2009-00778	FY09EM21-21	ccc	Measured	FY-09 Enhanced DOE HLW Melter Throughput Studies at SRNL	26.715	-13.042
SRNL-STI-2009-00778	FY09EM21-21	quenched	Targeted	FY-09 Enhanced DOE HLW Melter Throughput Studies at SRNL	29.960	-13.226
SRNL-STI-2009-00778	FY09EM21-21	quenched	Measured bc	FY-09 Enhanced DOE HLW Melter Throughput Studies at SRNL	30.154	-13.007
SRNL-STI-2009-00778	FY09EM21-21	quenched	Measured	FY-09 Enhanced DOE HLW Melter Throughput Studies at SRNL	30.156	-13.042

Figure 7 provides plots of the Al_2O_3, Fe_2O_3, Na_2O, and TiO_2 concentrations for these two groups of ComPro™ entries. A review of these results suggests that the concentrations of none of these individual oxides alone appear to lead to situations where the PCT response for boron is unpredictable by the THERMO™ model. Thus, the concentrations of combinations of oxides more than the concentration of an individual oxide appear to lead to unpredictable situations. Two major conclusions from this are:

1. The value of glass variability studies is reinforced. These studies are routinely conducted in support of the DWPF operation to ensure the operational feasibility of the sludge/frit glass systems studied and to validate the reliability of the THERMO™ models to predict the associated PCT responses.

2. Table 5 and Table 6 help to clearly define the region over which the durability models have been and are being studied. The ComPro™ results presented in this report demonstrate that the durability models have performed adequately for previously studied glasses from this region, which is defined by Table 8. However, there are limited data for TiO_2 above 2 wt% in Figure 7 and no Cs_2O data in Table 8. Of note is that all the replicates of the ARM-1 glass, a durability standard that contains 1.16 wt% Cs_2O that has been used in various durability studies, are not shown in Table 8. Also Cs_2O and K_2O act similarly in the DWPF THERMO™ model and there is coverage in K_2O space as well as in Cs_2O space in the historic THERMO™ database (see Table 2) which is imbedded in ComPro™.

It is recommended that for durability, which is a waste-form affecting property, confirmations of the performance of the associated models for specific, operationally-feasible glass composition regions (i.e., sludge batch/frit systems) via variability studies be continued. Moreover, the variability study is a requirement of the Glass Product Control Program.[90]

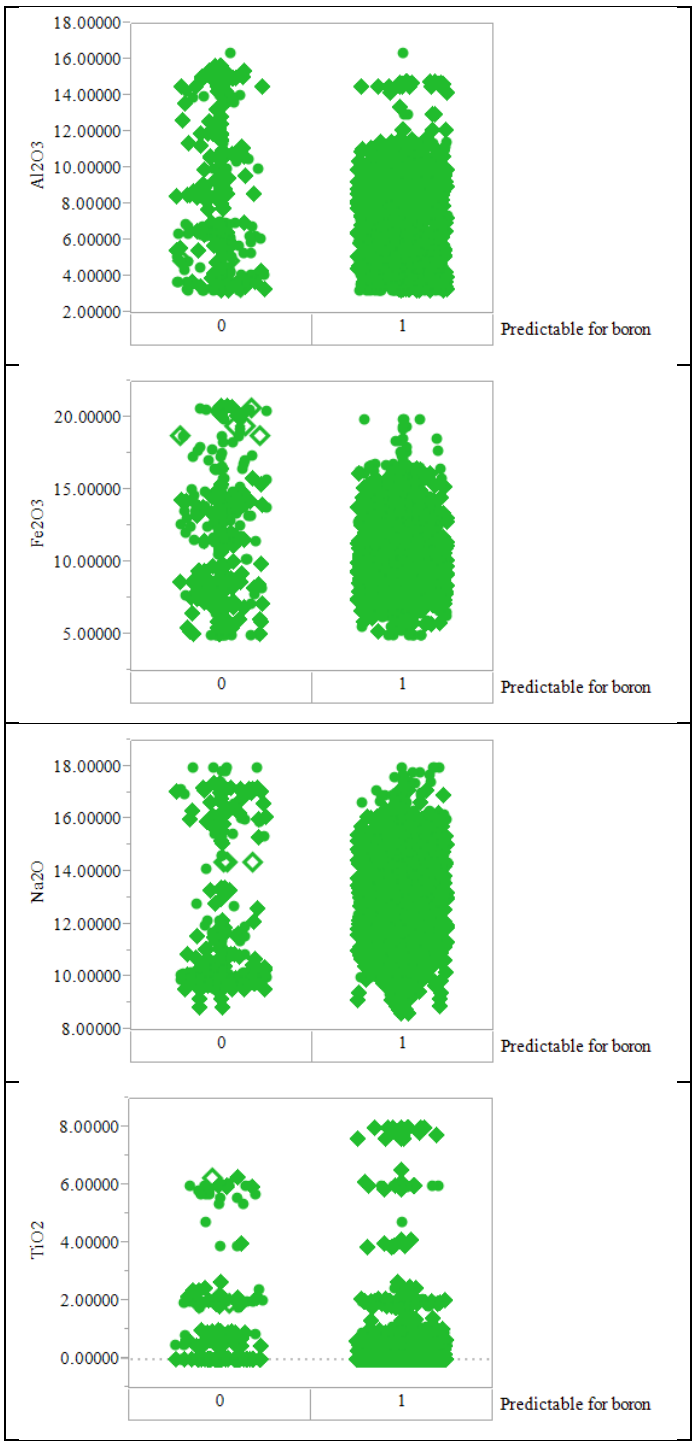

(0 => unpredictable; 1 => predictable)

Figure 7 Al_2O_3, Fe_2O_3, Na_2O, and TiO_2 wt% Concentrations for the ComPro™ Quenched and ccc Durability Entries

3.4 Assessment of PCCS Viscosity Model and Validation Ranges in DWPF Future Processing Range

The sources of the viscosity model and validation data as a function of measurement temperature and glass composition are given in Table 10. This includes the validation data used in 2005 and accumulated between 1991 and 2005 and the validation data accumulated between 2005 and 2014.

In addition to the constraints discussed for the DWPF durability model, the following constraints were added before the compositional constraints given in Figure 4[f] were applied. Note that constraints 2-5 are the same as those discussed in Appendix A for durability.

1. viscosities below 10 poise were not modeled as the ASTM 965 procedure can be inaccurate in this range of viscosity
   - if more than 2 out of 5 viscosity measurement points for a given glass as a function of temperature violated the 10 poise criterion then the entire set of glass viscosities was not considered for validation
2. no glasses with Al_2O_3 contents $\leq$ 3.00 wt% were included due to the potential for phase separation in the glass and anomalous viscosity behavior
3. no glasses with P_2O_5 contents $\geq$ 2.25 wt% (the DWPF solubility limit) were included due to the potential for phase separation in the glass and anomalous viscosity behavior
4. no glasses with B_2O_3 contents $\geq$ 14.00 wt% were included due to the potential for phase separation in the glass and anomalous viscosity behavior
5. no crystallized glasses nor glasses that crystallized during viscosity measurement, i.e. anomalous hysteresis curves were included as the viscosity measurement can be non-Newtonian
6. no glasses that had $Fe^{2+}/\Sigma Fe$ ratios outside the DWPF upper limit of 0.33 were included as highly reduced glasses have lower viscosities than their oxidized counterparts, which would require an FeO term in the DWPF viscosity model (and DWPF will never approach this upper limit due to other processing considerations).

The ability of the viscosity model to successfully predict the validation data that satisfied this screening process was evaluated. The 95% confidence intervals for individual predictions determined by JMP were used to conduct this evaluation. Table 11 provides summary statistics for the outcome of this evaluation: 86 results were not predictable and 583 results were predictable. On a percentage basis, more than 87% of these results were predictable by the current DWPF viscosity model. The table also provides a listing of the minimum and maximum values for each oxide for each category (i.e., predictable and not predictable) of outcomes.

The last two columns of Table 11 provide the range of the data over the viscosity model was evaluated as part of this study.

[f] For the viscosity model, the compositional constraints for both K_2O and MgO imposed by Figure 4 were modified to have upper bounds of 4 wt% and the lower bound on Fe_2O_3 was set at 4 wt% to provide broader compositional coverage and allow more data into this evaluation.

Table 10. References for Viscosity Model and Validation

Sample Study	Model or Validation	Viscosity-Temperature Measurements	Viscosity Data Year	Reference
Model Data	MODEL – Corning Engineering Laboratory Services (CELS) and Owens Corning Fiberglas-Sharp Shurtz (OCF-SS)	160	2005	19
DWPF Startup Frit	MODEL (OCF-SS)	15	2005	19, 91
DWPF Startup Frit	VALIDATION (Round Robin) Standards used in other studies	164 + 40	2005	19, 92, 93
Waste Form Compliance Plan (WCP) Glasses	VALIDATION	129	2005	19, 94, 95, 96, 97, 101, 104, 106
PNNL Studies (Chemical Variability Study; CVS-1 and CVS-2)	VALIDATION	699	2005	98
SRNL Integrated DWPF Melter System (IDMS) glass (Hanford, PX and HM)	VALIDATION	195	2005	19, 97
SRNL SGM	VALIDATION	331	2005	97
SRNL Soper (1982)	VALIDATION	124	2005	19, DPSTN-3345, DPSTN-4025, DPSTN-4416, 99
Crystalline SilicoTitanate (CST) Glasses	VALIDATION	70	2005	19, 100, 101, 102, 103, 104
Precipitate Hydrolysis Aqueous (PHA)	VALIDATION	74		19, 105, 106, 107, 108, 109
Environmental Assessment (EA) Glass	VALIDATION	7	2005	19, 44, 45
West Valley (WVCM and WVUTh, AL,CR,FE,MN, NI,P glasses)	VALIDATION	228	2005	19, 110, 111
M-Area	VALIDATION	80	2005	112
U and U/Th Glasses (RC, RCTH,Tank 40, rchwl, Glass 1-5 and U std)	VALIDATION	466	2005	19, 93, 96, 113
M-Area (compositions revised in 2014)	VALIDATION	80	2014	114
PNNL Study Glasses (SG)	VALIDATION	60	2014	115
Sulfate Glasses	VALIDATION	90	2014	116
High Loaded HLW Glasses	VALIDATION	264	2014	117, 118
CST/MST Glasses	VALIDATION	587	2014	119, 120, 121, 122
DWPF Non-Rad Startup Glasses (WP-14, 15, 16) as a Function of REDOX	VALIDATION	48	2014	123

Table 11. Viscosity Predictability as a Function of Glass Composition in Weight Percent for Validation Glasses

Oxide	Not Predicable		Predictable		Compositional Region Evaluated for Viscosity Model	
	86		583			
	min	max	min	max	min	max
Al_2O_3	4.114	14.551	3.255	14.551	3.255	14.551
B_2O_3	4.604	11.479	4.576	11.300	4.576	11.479
BaO	0.000	0.124	0.000	0.250	0.000	0.250
CaO	0.007	3.134	0.007	3.844	0.007	3.844
CdO	0.000	0.250	0.000	0.227	0.000	0.250
Ce_2O_3	0.000	0.360	0.000	0.348	0.000	0.360
Cr_2O_3	0.000	0.191	0.000	0.159	0.000	0.191
Cs_2O	0.000	0.129	0.000	0.126	0.000	0.129
CuO	0.000	0.058	0.000	0.450	0.000	0.450
Fe_2O_3	4.057	20.230	4.057	20.159	4.057	20.230
K_2O	0.000	2.700	0.000	3.860	0.000	3.860
La_2O_3	0.000	0.357	0.000	0.420	0.000	0.420
Li_2O	2.995	6.612	2.452	6.792	2.452	6.792
MgO	0.008	2.070	0.008	2.562	0.008	2.562
MnO	0.255	4.512	0.193	3.811	0.193	4.512
MoO_3	0.000	0.000	0.000	0.200	0.000	0.200
Na_2O	9.082	17.052	9.000	16.951	9.000	17.052
Nb_2O_5	0.000	0.081	0.000	0.444	0.000	0.444
N_bO_2	0.000	0.076	0.000	0.417	0.000	0.417
Nd_2O_3	0.000	0.000	0.000	0.390	0.000	0.390
NiO	0.006	2.392	0.006	2.341	0.006	2.392
P_2O_5	0.000	0.000	0.000	0.432	0.000	0.432
PbO	0.000	0.185	0.000	0.190	0.000	0.190
SO_4	0.000	0.486	0.000	0.904	0.000	0.904
SiO_2	40.379	50.790	40.433	52.600	40.379	52.600
SrO	0.000	0.000	0.000	0.035	0.000	0.035
ThO_2	0.000	0.000	0.000	0.057	0.000	0.057
TiO_2	0.120	6.213	0.000	7.740	0.000	7.740
U_3O_8	0.000	1.460	0.000	4.980	0.000	4.980
UO_2	0.000	1.404	0.000	4.791	0.000	4.791
ZnO	0.000	0.134	0.000	0.485	0.000	0.485
ZrO_2	0.000	0.356	0.000	0.499	0.000	0.499

Figure 8 provides plots of the Al_2O_3, Fe_2O_3, Na_2O, and TiO_2 concentrations for these two groups of viscosity outcomes. A review of these results and those of Table 11 suggests that the concentrations of none of these individual oxides alone appear to lead to situations where the viscosity response is unpredictable by the current model. Thus, the concentrations of combinations of oxides more than the concentration of an individual oxide appear to lead to unpredictable situations.

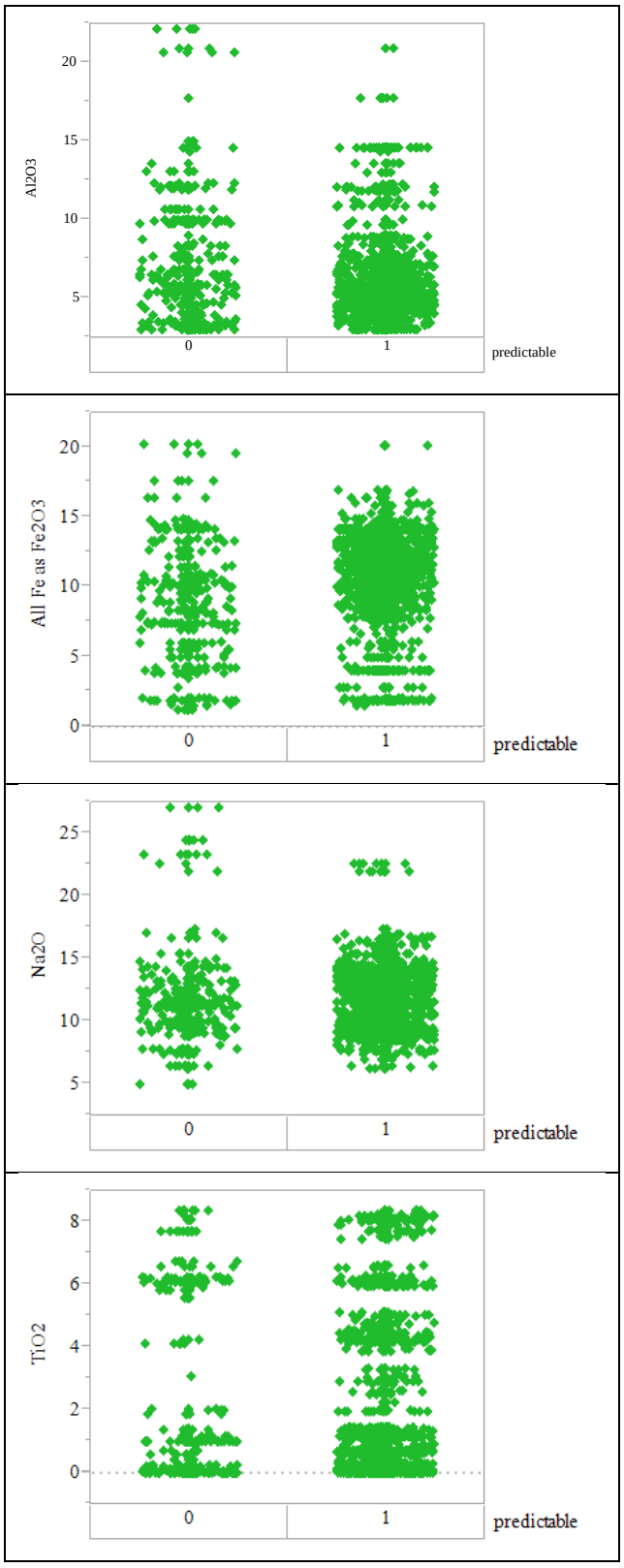

Figure 8 Al_2O_3, Fe_2O_3, Na_2O, and TiO_2 wt% Concentrations for the Viscosity Validation Data.

3.5 Assessment of PCCS Liquidus Model and Validation Ranges in DWPF Future Processing Range

Phase separation in glasses has been found to promote homogeneous nucleation and precipitation. Phase separation has been found to decrease the crystallization activation energy (*E*) and change the mechanism of crystallization of glasses.[38] Therefore, phase separated glasses are not used to model the liquidus temperature (T_L) or to validate the liquidus model. These are the same B_2O_3, P_2O_5, and crystallization constraints imposed upon durability and viscosity and discussed in Appendix A.

Table 12 gives the references for the PCCS liquidus model data (105 glasses) and the data available for model evaluation (113 glasses) generated in crucibles and one additional data point (1 glass) generated in a pilot scale melter. Since the T_L is a difficult measurement to make, this PCCS property has only these two usable datasets for model evaluation. However, when these results were screened by the compositional constraints of Figure 4 and even the more inclusion constraints utilized in the evaluation of the viscosity model, none of the available T_L results were found to be in the compositional region of interest in this study. Other datasets that could not be used for T_L model evaluation are discussed in Appendix D.

Table 12. References for Liquidus Model and Validation

Sample Study	Data Type	Measurement Laboratory	Measurement Method	T_l Measurements Total	Ref.
Model Data	MODEL	½ SRNL/CELS ½ PNNL	ASTM C829 ASTM C1720	105	22,23, 24
Small Cylindrical (SCM-2) Melter	VALIDATION	SRNL	Melter	1	23
Hanford High-Iron Tank Waste (SP, MS, US, MISC)	VALIDATION	PNNL	ASTM C1720	113	22, 124

Since no data in the region of interest for DWPF's future operation are available, this reinforces the value of the SWPF Gap analysis glass study [32] to provide liquidus temperature measurements for glasses that cover the compositional region of Table 6.

4.0 Conclusions

The modeling and validation regions for each of the PCCS models that are currently in use for DWPF processing were assessed in this document. The tables in this document, include (1) the model ranges over which the DWPF PCCS models were developed and (2) assessments of the PCCS models against newly available validation data accumulated since the models were developed or revised[ξ]. These tables show the individual oxide ranges for glasses that fit and do not fit the models at associated confidence intervals. These individual oxide ranges for predictable and non-predictable outcomes are shown to overlap.

The parsimonious nature of the DWPF PCCS models excludes composition terms that were unnecessary to the implementation of the DWPF flowsheet over the last 19 years. However, validation data have been collected over the intervening years through the use of variability studies and glass composition studies at SRNL and various other institutions. In this study, the PCCS models are assessed against two decades of additional durability data compiled in the COMPRO™ database and additional viscosity and liquidus data that has been generated since the 2005 viscosity model and 2001 liquidus model revisions: these validation data have been evaluated in individual studies but not collectively assessed.

The assessment of the PCCS models over the SWPF composition space is a prerequisite to a follow-on and more in-depth assessment of whether the PCCS models may require additional oxide components or parameters[f] or whether the weighting factors of the current oxide components or parameters need to be adjusted to cover the composition ranges anticipated. Both the prerequisite assessment and the follow-on in depth assessment will also determine whether additional species or parameters are needed to encompass any changes in frit formulation that may be necessary, e.g. MgO and/or CaO to prevent nepheline crystallization.

For the SWPF processing range, there are some data available to evaluate the viscosity model and durability model. For the liquidus model, there are no currently available data that fall in the SWPF composition region. Thus, compositional coverage is needed for the liquidus model. For the durability model, while Cs_2O concentrations up to a maximum of 1.16 wt% were tested during the development of the model in 1995, there are limited new data to assess the Cs_2O partial molar free energy effects. Also, there are limited data for TiO_2 concentrations above 2 wt%.

The prerequisite assessment indicates that a combined XO_2 term be added to the viscosity model to incorporate TiO_2, NbO_2, ZrO_2 and ThO_2, which should all have a similar structural impact on the glass viscosity. It is also recommended that a combined XO term be added to the viscosity model to encompass CaO and MgO, which may be needed as additional frit components to minimize or prevent nepheline crystallization. Terms for TiO_2, NbO_2, ZrO_2, ThO_2, CaO and MgO are in the durability model but have not been vetted with much of the additional validation data that has been compiled over the last 19 years. Terms for TiO_2, ZrO_2, CaO, and MgO are in the liquidus model but have not been vetted with additional liquidus data. This vetting against newly derived liquidus data may require that the parameter coefficients be refitted. The results for the viscosity and liquidus models reinforce the value of the SWPF Gap analysis glass study to provide property measurements for glasses that cover the compositional region of Table 6.

ξ Validating data over wider composition ranges as presented in Appendices B, C, and D indicate that a smaller percentage of the data fit the DWPF modeling space compared to validating over DWPF like SWPF space, which is anticipated.

f Where a parameter is defined as a group of oxides, like the alkali oxides of Cs, Na, K, and Li, that act as a grouped parameter in a model.

Lastly, the durability model may require a modification to the way in which the normalized leaching parameter is calculated based on the ASTM C1285 (Product Consistency Test) procedure. The ASTM C1285 procedure requires that the glass durability be calculated using the glass density. For higher waste loaded glasses, which are denser, a smaller SA would be calculated compared to a nominal waste loaded glass, and this has an inverse impact on the normalized release, i.e. it would be biased higher as observed for the higher waste loaded glasses examined in the DWPF future processing range(s). Moreover, the bias in the high waste loaded glasses, in terms of their durability response, may be related to a ratio used in the commercial glass industry, the $SiO_2/(Na_2O+B_2O_3$ ratio). Below a critical ratio of 0.333, there is always an interconnected path of non-bridging glass forming sites that can deteriorate the durability of a glass. Both the density and the $SiO_2/(Na_2O+B_2O_3$ ratio) need to be investigated during the in-depth analysis to be performed on the DWPF PCCS models before SWPF startup.

Table 13. PCCS Model Predictability Assessed Over DWPF Future Processing Ranges

Model	Validation Data Predictability
Durability – based on B release prediction	90%
Viscosity – based on all temperatures (not just 1150°C)	87%
Liquidus	no applicable data available

5.0 Acknowledgements

The authors would like to acknowledge the assistance of Scott Reboul of Savannah River National Laboratory in calculating the radionuclides from the pour stream samples for Table 2.

APPENDIX A. Modeling Constraints

As stated in Section 2.1, various constraints on the compositions of glasses being considered for inclusion in modeling must be applied. The sum of oxides (100±5 wt%) was mentioned above, as well as the importance that a given glass must be homogeneous, i.e. not phase separated by liquid-liquid amorphous phase separation (APS) due to low Al_2O_3 (≤3.00 wt%), high P_2O_5 (≥2.25 wt%), or high B_2O_3 (≥15.00 wt%) concentrations. The impacts of low Al_2O_3, high P_2O_5, or high B_2O_3 on glass durability are discussed below.

A.1 The Homogeneity and Low Al_2O_3 Constraint

A homogeneity constraint was developed as part of THERMO™ to ensure that DWPF glasses were homogeneous.[20,21] It was noted during the development of THERMO™ that a minimum of 3 wt% Al_2O_3 was necessary in high Fe_2O_3 containing and high Na_2O containing glasses to avoid amorphous phase separation.[20,21,63] Amorphous phase separation in low Al_2O_3 containing glasses is consistent with the known immiscibility gap in the Al_2O_3-Fe_2O_3-Na_2O-SiO_2 quaternary system that defines the melt surface and crystallization of molten basalt magmas.[125] It is also consistent with known phase separation in Na_2O-Al_2O_3-SiO_2 glasses that are known to phase separate when the glasses contain less than ~ 3 wt% Al_2O_3.[126,127]

The homogeneity constraint was implemented in the DWPF PCCS to avoid the possible production of glasses that could be phase separated (liquid-liquid phase separation) and not predictable by the durability models. While the homogeneity constraint was typically an issue at lower waste loadings (WLs), it may impact the operating windows[ξ] for DWPF operations, where the glass forming systems may be limited to lower waste loadings based on fissile or heat load limits. In the Sludge Batch 1b (SB1b) variability study, application of the homogeneity constraint at the MAR limit eliminated much of the potential operating window for DWPF.[128] As a result, Edwards and Brown [129] developed criteria that allowed DWPF to relax the homogeneity constraint from the MAR to the property acceptance region (PAR), which opened up the operating window for DWPF operations. These criteria are defined as:

(1) use the alumina constraint as currently implemented in PCCS ($Al_2O_3 \geq 3$ wt%) and add a sum of alkali constraint with an upper limit of 19.3 wt% ($\sum R_2O < 19.3$ wt%), or

(2) adjust the lower limit on the Al_2O_3 constraint to 4 wt% ($Al_2O_3 \geq 4$ wt%).

where $\sum R_2O$ is the sum of the concentrations of the alkali oxides, i.e. $Cs_2O+K_2O+Li_2O+Na_2O$. The alkali and alumina limits in criterion 1 above are those of the Waste Form Compliance Plan (WCP) Purex glass and the criteria are not only to ensure that glasses are not phase separated but to ensure that the glass durability stays well below that of the benchmark EA glass. Recent studies on the long term durability of high alkali versus low alkali glasses has shown that high alkali glasses return to the undesirable accelerated rate of dissolution preferentially to low alkali glasses.[130, 131] Therefore, the implementation of an alkali/alumina constraint for DWPF glasses was prudent.

Historical glasses of interest to DWPF meeting criteria 1 and 2 above were found to be acceptable using a normalized boron release (NL [B]) of 10 g/L as a benchmark. This value was chosen in order to be certain that the boron releases of the study glasses were well below that of the EA glass with measurement and analytical uncertainty considered. It should be emphasized that this limit was not empirically derived and was only used as a guide to develop the Al_2O_3 and/or sum or alkali criteria.

[ξ] The WL interval over which a particular glass system is considered to be acceptable based on model predictions.

Herman et al. [132] later demonstrated that these criteria could be used to replace the homogeneity constraint for future sludge-only batches.

In addition to variability studies, other studies [82] were conducted to better understand the homogeneity-composition relationship, which is discussed next. Raszewski and Edwards [82] conducted a reduction of constraints (ROC) study for coupled operations and this is discussed in Section 3.1.

A2.1 High P_2O_5 Constraint

Glasses were further screened for modeling (see Figure 1) and were not modeled if they contained >2.25 wt% P_2O_5 (Figure 1) as this had been shown to cause lithium phosphate phase separation and compromise glass durability.[133,134,135] High P_2O_5 (>2.25 wt%) concentration creates crystalline phosphate phases by crystalline phase separation (CPS). In CPS the two phases, one phosphate rich, co-exist as liquid phases in the melt and the glass cannot be quenched rapidly enough to prevent the phosphate rich liquid from crystallizing.[134,135]

A2.2 High B_2O_3 Constraint

In 1994 Tovena, et. al. [34] demonstrated that various glass durability models, whether based on thermodynamics, enthalpy or structural concepts, did not predict waste glass durability accurately when the composition of the waste glass contained >15% B_2O_3 with little or no Al_2O_3. For these glasses, all the models under-predicted the glass durability significantly. Tovena, et. al. [34] attributed the under prediction to phase separation and complete dissolution of a borate rich phase in the glass when the Al_2O_3 content was insufficient. This was confirmed by SRNL researchers in 1995 [20,21,63] and a B_2O_3 constraint of 14 wt% is imposed to be conservative.

A2.3 Crystallization Constraint

Crystallization can impact durability in several ways as shown in Equation 1. For homogeneous glasses, it has been shown that B release is congruent with the ^{99}Tc dissolution.[48-58] As long as ^{99}Tc does not partition into a given crystalline phase, this relationship will hold. If ^{99}Tc partially partitions into a crystalline phase, then there would be a durability vector from both the glass and the crystal. In addition, one would have to consider whether release of ^{99}Tc from the glass was accelerated from the grain boundary around the crystal since the crystal can deplete the surrounding glass of certain glass forming components. If ^{99}Tc partitioned completely into a crystalline phase, then there would be a durability vector only from the crystal and the equivalency of ^{99}Tc release to B release would no longer hold.

Spinel crystallization has been found not to accelerate grain boundary dissolution because it is isotropic and so is the waste glass. Spinel does not sequester any radionuclides and only sequesters transition metals from the waste and so spinel crystallization impacts are virtually non-existent.[36,136] Therefore, no constraint exists for spinel crystallization.

Nepheline has been found to have a strong impact on durability and acmite a moderate impact on durability.[136] Acmite sequesters mostly transition metals from the waste and no acmite constraint exists. However, nepheline sequesters glass formers from the matrix glass and, thus, accelerates grain boundary dissolution (see Equation 1). While nepheline does not sequester ^{99}Tc, it may sequester ^{137}Cs and nepheline crystallization in a nuclear waste glass canister is, therefore, minimized during processing by processing glass compositions that are unfavorable to nepheline formation. This additional constraint, the nepheline constraint, was defined by Li et. al. [137,138] and implemented in DWPF by Edwards, Peeler, and Fox [139].

APPENDIX B. 1995 DWPF THERMO™ Durability Model and Validation Ranges

During development of THERMO™, it was determined that a minimum of 3 wt% Al_2O_3 was necessary in Fe_2O_3 and Na_2O containing glasses to avoid phase separation [63]. Since the alumina constraint was found during model development, there are a few glasses in THERMO™ [20,21] that contained <3.0 wt% Al_2O_3, i.e. specifically 5 glasses out of 132 glasses or 3.8% of the population of THERMO™ model data. The WCP Purex glass has an Al_2O_3 concentration of 2.99 wt% , but it was determined to be homogeneous. In addition, a PCT round robin was performed on the WCP Purex glass [95] and it was determined to have an acceptable durability.

Several glasses in THERMO™ went beyond the alkali/alumina constraint that was implemented after development of the model because (1) the model included high alkali glasses such as the EA (21.1 wt% alkali oxides) glass and (2) all the DWPF models were developed over wider composition ranges than the implementation range. If the EA glass is excluded, there are only 7 of the 132 glasses in THERMO™ that went beyond the alkali/alumina constraint. Five of the 7 glasses that go beyond the alkali/alumina criteria are the same ones that were predicted to be phase separated, i.e. only 5.3%.

No crystallized glasses were used as model data in THERMO™. Glasses were also screened to ensure congruent leachate analyses. There were 132 glasses in "Model Data" with 396 PCT responses as most glasses were tested in triplicate by the ASTM C1285 procedure.[46]

There were 348[f] glasses in THERMO™ validation data of which 310 glasses were predictable and 38 glasses were not, i.e. 89% of the validation data fit the THERMO™ model. The THERMO™ validation data included glasses made in crucibles and glasses made in large pilot scale melters. In addition, data from full scale canisters poured during the non-radioactive startup of the DWPF at the SRS during Qualification Runs (sections and grab samples from Facility Acceptance FA-13, Waste Processing WP-14, and Waste Processing WP-15). Each of these glasses was tested in triplicate PCT.

Table 14 gives the ranges of the THERMO™ "Model Data" and the THERMO™ "Validation Data" from Reference 21 for glasses falling within the upper 95% confidence bands (U95) and the lower 95% confidence band (L95) of the THERMO™ model (labelled "predictable"). In addition, the "Validation Data" for glasses falling outside the U95 and L95 confidence bands of the THERMO™ model are given in Table 14 (labeled "not predictable"). A review of the results in Table 14 demonstrates that the individual oxide ranges overlap because, mechanistic models cover a continuous property space and not a continuous oxide composition space. Mechanistic models take advantage of interactions between individual oxide terms where appropriate and their coupled impact on a given glass property, i.e., all alkali break two bonds in the PCCS viscosity model. This allows the property space to be continuous and account for multiple interactions. . However, the large majority of the 38 glasses not predictable by the THERMO™ model in Table 14 contained $B_2O_3 \geq$ 14 wt%, which according to Tovena [34] are phase separated. A large proportion of the remaining non-predictable glasses were high in total alkali (Σalkali>19.3 wt%) or low in Al_2O_3 ($\leq$ 3 wt%) and would not have passed the alkali/alumina constraint now imposed on DWPF glass durability. [82,129,132] Several non-predictable glasses were extremely high in Al_2O_3 (>20 wt%).

[f] Table V in THERMO™ says 346 validation data but there is an error in the DWPF WP-15 count which should be a total of 104 glasses of which 102 glasses were used.

Table 14. Composition Ranges (wt%) for the DWPF Durability Model (THERMO™) and Validation Data

Species in THERMO™	THERMO™ Durability Model (132 glasses; 396 PCT measurements)	THERMO™ Validation (348 glasses; >1000 PCT Measurements		DWPF Pour Stream Glass Ranges SB1a-SB7b (See Appendix E)
		310 glasses (~930 PCT measurements) Predictable	38 glasses (~114 PCT measurements) NOT Predictable	
$Fe^{+2}/\Sigma Fe$ ratio	0.00-1.29	0.00-0.25	0.00-0.21	0.00-0.38
Al_2O_3	1.36‡-13.90	2.56-16.77	0.56-22.80	3.57-9.83
B_2O_3	6.10-13.30	4.30-15.95	4.70-21.19	4.27-9.06
BaO	0.00-0.66	0.00-0.16	0.00-0.19	0.00-0.06
CaO	0.38-2.23	0.00-8.68	0.00-8.20	0.43-1.39
Ce_2O_3	0.00-1.44	0.00-0.02	0.00-0.02	0.00-0.07
Cr_2O_3	0.00-0.55	0.00-0.86	0.00-0.37	0.00-0.16
Cs_2O	0.00-1.16	0.00-0.18	0.00-0.26	0.00
CuO	0.00-0.33	0.00-0.54	0.00-0.53	0.00-0.63
Cu_2O	0.00-0.30	0.00-0.48	0.00-0.48	0.00
FeO	0.00-8.81	0.00-2.52	0.00-2.57	0.00-2.99
Fe_2O_3	0.00-14.30	0.00-20.77	0.00-19.40	5.42-12.56
$(\Sigma Fe)_2O_3$	0.00-17.42	0.00-22.45	0.00-22.25	8.21-12.56
K_2O	0.00-5.73	0.00-5.25	0.00-7.22	0.00-1.8
La_2O_3	0.00-0.42	0.00-0.22	0.00	0.00-0.04
Li_2O	2.59-5.16	0.00-5.41	0.00-5.38	3.53-5.55
MgO	0.00-3.24	0.00-2.08	0.00-3.79	0.22-2.16
MnO	0.00-3.36	0.00-3.56	0.00-5.09	1.11-2.44
MoO_3	0.00-1.67	0.00-0.11	0.00-0.02	0.00-0.04
Na_2O	6.42-16.80	4.67-24.43	4.26-22.28	11.05-14.86
$\Sigma(Cs_2O+K_2O+Li_2O+Na_2O)$	13.09-21.10	12.59-24.43	10.46-23.54	15.03-19.3
Nd_2O_3	0.00-5.96	0.00-0.42	0.00-0.03	0.00
NiO	0.00-2.97	0.00-1.77	0.00-2.57	0.00-1.38
P_2O_5	0.00-0.65	0.00-0.59	0.00-0.59	0.00-0.63
PbO	0.00-0.25	0.00-0.21	0.00-0.28	0.00-0.16
SiO_2	39.80-59.80	40.28-62.71	38.72-63.75	44.77-54.60
SrO	0.00-0.45	0.00-0.05	0.00-0.01	0.00-0.32
ThO_2	0.00	0.00	0.00	0.00-1.00
TiO_2	0.00-3.21	0.00-0.88	0.00-1.05	0.00-0.66
U_3O_8	0.00	0.00	0.00	0.00-3.51
ZnO	0.00-1.46	0.00-0.42	0.00-0.14	0.00-0.09
ZrO_2	0.00-1.80	0.00-2.48	0.00-1.	0.00-0.62

‡ During development of THERMO™ it was determined that a minimum of 3 wt% Al_2O_3 was necessary in high Fe_2O_3 containing and high Na_2O containing glasses to avoid phase separation [63]. This is consistent with the known immiscibility gap in the Al_2O_3-Fe_2O_3-Na_2O-SiO_2 quaternary system that defines the crystallization of basalt [125].

* During development of glass durability models, glasses with P_2O_5 values in excess of 2.25 wt% were shown to exhibit crystalline phase separation (CPS) [133,134,135].

APPENDIX C. VISCOMP™ Viscosity Model and Validation Ranges

The VISCOMP™ database (see [18] and [19]) was used in addition to the information and results of additional validation data given in Table 10 to investigate the range of validity for the viscosity model for future DWPF processing. The outcome of this investigation is presented in Section 3.4. A broader look at the compositional ranges covered by the viscosity model and validation data is given in this appendix and covers compositional regions outside of the regions defined in Table 5 and Table 6.

The validation data used in 2005 included ~200 replicate viscosity measurements on the DWPF startup frit by six different laboratories, ~130 measurements on the WCP glasses by Owens Corning Fiberglass/ Sharp-Shurtz(OCF/SS), ~10 measurements of the EA glass by OCF/SS, ~140 glasses from West Valley measured at Alfred University, ~125 measurements from SRNL testing in the early 1980's, ~700 measurements from Pacific Northwest National Laboratory (PNNL) on two different statistically designed matrices of simulated waste glasses (Composition Variability Study I and II), and ~530 measurements made by OCF/SS on glasses made in the SRNL Integrated DWPF Melter System (IDMS) and the Scale Glass Melter (SGM). A data set of 192 radioactive viscosity-temperature pairs containing only U^{+6} was assessed against the revised non-radioactive DWPF viscosity model. While U^{+6} appears to have little to no impact on glass viscosity, this may or may not be true for U^{+4} and U^{+5} in glass since these species were not examined in the 2005 study. This is of especial note since the DWPF is currently operating at a REDOX target of 0.2 where 45% of the uranium is U^{+6}, 45% is U^{+5}, and 10% is U^{+4}. An additional 26 glasses for which 98 viscosity-temperature measurements were available indicate disparate roles for ThO_2 depending on the U_3O_8 concentration and the Al_2O_3 concentration of the glasses measured. These datasets and results are all documented in reference 19.

The 2005 viscosity model revision is based on 33 of the original 1991 waste glasses and pure frits. The measured composition data ranges for these glasses are shown in Table 15. The modeling and validation ranges for the 2005 DWPF viscosity model are also given in Table 15 from reference 19.

Of the 1805 non-radioactive glass viscosity-temperature-compositions available for validation of the DWPF model in 2005, about 801 were eliminated on the following basis:

- if the measured composition was <95 wt% or >105 wt% on an oxide basis, the analysis was considered inadequate for validation
- if the measured temperature was ≤800°C, the data were excluded to avoid bias due to potential non-Newtonian viscosity behavior due to crystallization below 800°C

In order to constrain the validation data examined in 2005 to a composition range that overlapped the DWPF composition range but was, in general broader, while not having to develop new composition terms for ZrO_2, CaO, MgO or other components (all are known to impact glass viscosity strongly), the following boundary conditions were set:

- if the ZrO_2 was ≥2.00 wt%, which was twice the ZrO_2 content of the data on which the DWPF model is based (see Table 15), the data were excluded
- if the CaO was ≥3.5 wt%, which was more than twice the CaO content of the data on which the DWPF model is based (see Table 15), the data were excluded
- if the MgO was ≥6.00 wt%, which was twice the MgO content of the data on which the DWPF model is based (see Table 15), the data were excluded
- if the B_2O_3 was ≥14.00 wt%, which was over the B_2O_3 content of the data on which the DWPF model is based (see Table 15) by 2 wt% but likely in the range of phase separated glasses as defined by Tovena [34], the data were excluded.

Table 15. Temperature, Viscosity and Composition Ranges for the DWPF Viscosity Model

Parameter	1991-2005			2005-2014	1991-2014	1991-2014	DWPF Pour Stream Composition SB1a-SB7b (1996-2014) (compositions from Appendix E; calculated viscosity from 2005 PCCS model)
	Viscosity and Resistivity "Model Data" (33 glasses; 175 viscosity-temperature pairs)	Non-Radioactive Validation (170 glasses; 1004 viscosity-temperature pairs)	Radioactive Validation U_3O_8 Glasses Only Ranges (45 glasses; 192 viscosity-temperature pairs)	Non-Radioactive Validation (113 glasses; 727 viscosity-temperature pairs)	Composite Non-Radioactive and Radioactive Ranges (247 glasses; 1827 viscosity-temperature pairs)	Composite Non-Radioactive and Radioactive Ranges (48 glasses; 335 viscosity-temperature pairs)	
	MODEL DATA	PREDICTED	PREDICTED	PREDICTED	PREDICTED	NOT PREDICTED	
Temperature (°C)	873-1491	803-1350	974-1258	902-1352	808-1352	827-1304	1150
Viscosity (poise)	10.2-1,122.02	8.9-11,000	10.8-7,979.51	10-1,206.90	10-11,000	10.6-4,900.00	40.3-79.0
$Fe^{+2}/\Sigma Fe$	0.00-0.47	0.00-0.71	0.00	0.00-0.24	0.00-0.24	0.00	0.00-0.38
Al_2O_3(wt%)	0.00-13.90	0.81-17.74	2.53-29.02	3.25-12.52	2.99-20.70	2.99-15.00	3.57-9.83
B_2O_3(wt%)	6.41-12.20	4.90-13.25	4.33-11.89	3.85-12.97	3.85-13.25	4.13-13.05	4.27-9.06
BaO(wt%)	0.00-0.20	0.00-0.50	0.00	0-0.78	0.00-0.78	0.00-0.50	0.00-0.06
CaO(wt%)	0.00-1.47	0.02-3.2	0.29-1.79	0.01-5.58	0.01-7.60	0.01-10.20	0.43-1.39
Cr_2O_3(wt%)	0.00-0.09	0.00-1.18	0.07-0.30	0.00-0.43	0.00-0.69	0.00-0.26	0.00-0.16
Cs_2O(wt%)	0.00-0.15	0.00-0.67	0.00	0.00	0.00-0.28	0.00-0.17	0.00
CuO(wt%)	0.00-0.33	0.00-0.10	0.00-0.51	0.00-0.48	0.00-1.02	0.00-0.20	0.00-0.63
Cu_2O(wt%)	0.00-0.30	0.00-0.82	0.00-0.46	0.00	0.00	0.00	0.00
FeO(wt%)	0.00-7.14	0.00-0.24	0.00	0.00-2.72	0.00-2.72	0.00	0.00-2.99
Fe_2O_3(wt%)	0.00-14.20	0.00-0.23	1.74-16.86	5.80-20.23	1.55-20.16	1.9-20.23	5.42-12.56
K_2O(wt%)	0.00-5.73	0.00-0.20	0.00-5.84	0.00-15.83	0-15.83	0.00-15.14	0.00-1.80
La_2O_3(wt%)	0.00-0.36	0.00-8.62	0.00	0.00-0.13	0-2.12	0.00-0.79	0.00-0.04
Li_2O(wt%)	2.59-6.96	1.90-17.74	0.00-6.82	1.19-7.32	0.00-7.32	1.39-6.61	3.53-5.55
MgO(wt%)	0.49-2.92	0.00-4.80	0.06-2.47	0.01-2.56	0.00-7.71	0.00-7.15	0.22-2.16
MnO(wt%)	0.00-3.26	0.03-3.31	0.03-4.02	0.25-3.81	0.02-4.02	0.01-4.61	1.11-2.44
Na_2O(wt%)	5.80-15.80	6.41-16.8	7.27-12.74	6.26-17.05	6.26-23.35	5.04-24.50	11.05-14.86
Nb_2O_5 (wt%)	0.00	0.00	0.00	0.00-2.90	0.00-2.90	0.00-2.51	0.00
NiO(wt%)	0.00-2.97	0.00-3.01	0.19-2.78	0.01-2.34	0.01-2.78	0.01-2.59	0.00-1.38
P_2O_5 (wt%)	0.00	0-1.01	0-0.76	0.00	0.00-1.56	0.00-1.05	0.00-0.63
SiO_2(wt%)	45.60-77.04	40.50-60.39	34.15-55.85	36.90-55.67	36.90-60.39	39.78-55.30	44.77-54.60
SrO(wt%)	0.00-0.07	0.00-0.18	0.00-0.06	0.00	0.00-0.18	0.00-0.14	0.00-0.32
ThO_2 (wt%)	0.00	0.00	0.06	0.00-0.62	0.00-3.90	0.00-2.66	0.00-1.00
TiO_2(wt%)	0.00-1.78	0.00-1.43	0.00-3.10	0.00-8.38	0.00-8.38	0.00-7.71	0.00-0.66
U_3O_8 (wt%)	0.00	0.00	0.00-5.76	0.00-5.22	0.00-5.76	0.00-3.08	0.00-3.51
ZnO(wt%)	0.00	0.00-0.21	0.00	0.00-0.14	0.00-0.49	0.00-0.13	0.00-0.09
ZrO_2(wt%)	0.00-0.99	0.00-2.00	0.00-0.97	0.00-2.43	0.00-4.40	0.00-3.52	0.00-0.62

Since the current evaluation of the models is to investigate model range applicability, the restrictions on ZrO_2, CaO, and MgO were not applied but the following restraints were retained:

- sum of oxides
- no temperature ≤800°C to avoid data bias due to crystallization

In addition, the following constraints were added before the values in Table 15 were generated.

- no viscosities below 10 poise as the ASTM 965 procedure can be inaccurate in this range of viscosity
    - if more than 2 out of 5 measurement points violated the 10 poise criteria then the entire set of glass viscosities was not considered for validation
- no Al_2O_3 contents ≤ 2.99 wt% due to the potential for phase separation in the glass and anomalous viscosity behavior
- no P_2O_5 contents ≥ 2.25 wt% due to the potential for phase separation in the glass and anomalous viscosity behavior
- no B_2O_3 contents ≥ 14.00 wt% due to the potential for phase separation in the glass and anomalous viscosity behavior
- no crystallized glasses nor glasses that crystallized during viscosity measurement, i.e. anomalous hysteresis curves, were used as viscosity is non-Newtonian
- no glasses that had $Fe^{2+}/\Sigma Fe$ ratios outside the DWPF upper limit of 0.33 as highly reduced glasses have lower viscosities than their oxidized counterparts, which would require an FeO term in the DWPF viscosity model when DWPF will never approach this upper limit due to other processing considerations

Many of these constraints are those already introduced in Figure 1.

Therefore, the viscosity validation data from 1991-2014 are assessed as a pooled group after the individual non-radioactive and radioactive glass studies are assessed. In Table 15, it can be seen that the individual ranges of the oxides overlap for those glasses that do fit the 2005 viscosity model and those glasses that do not fit the 2005 viscosity model. There is a pool of 295 validation glasses listed in Table 15. Only 48 glasses do not fit the current PCCS viscosity model (Table 15) and most of these glasses have high CaO (up to 10.20 wt% CaO) compared to the glasses that do fit the viscosity model (up to 7.60 wt% CaO).

The vast majority (~84%) of the validation glasses (295 glasses) fit the DWPF viscosity model over much wider ranges than it was developed. The percentage would be 87% predictable if the CaO term were constrained to ≤ 3.50 wt% CaO as done in the 2005 viscosity model validation study where CaO was truncated at twice the values of model data the 87% of the glasses were predictable and 13% were not.[19] If the glasses are further screened for MgO≥ 6.00 wt%, as done in the 2005 model validation, then 87% are still predictable.

In model data, only one of the 33 glass datasets did not fit the model well. Therefore, a pooled set of 295+33=328 glasses was available for analysis of which 49 glasses were not predictable. Over a broader range than assessed using the values in Table 5 and Table 6, the DWPF viscosity model gives a prediction capability of 85%. If the high CaO and MgO data are screened at 3.50 and 6.0 wt% respectively, then the prediction capability improves to 89%.

APPENDIX D. LIQCOMP™ Liquidus Model and Validation Ranges

The LIQCOMP™ database (see [22] and [23,24]) was used in addition to the information and results of additional validation data to investigate the range of validity for the liquidus model for future DWPF processing. The outcome of this investigation is presented in Section 3.5. A broader look at the compositional ranges covered by the liquidus model and validation data is given in this appendix (Table 16 and Table 17) and covers compositional regions outside of the regions defined in Table 5 and Table 6. Table 16 gives the references for the PCCS liquidus model data (105 glasses) and for potential validation data. Since the T_L is a difficult measurement to make, this PCCS property had only two usable validation datasets and this will be discussed below.

Phase separation in glasses has been found to promote homogeneous nucleation and precipitation. Phase separation has been found to decrease the crystallization activation energy (*E*) and change the mechanism of crystallization of glasses.[38] Therefore, phase separated glasses should not be used to model the liquidus temperature (T_L) or to validate the liquidus model. However, the LIQCOMP™ model data given in Table 17 indicates that several glasses that could potentially be phase separated, i.e. glasses with Al_2O_3 $\leq$3.00 wt%, and indeed as low as 0.99 wt%, were used in model development without any impact indicating that Al_2O_3 may not play a strong role in the crystallization of $NiFe_2O_4$ spinel.

Of the glasses that could not be used to validate the liquidus model, 24 were West Valley glasses that were measured isothermally to the nearest 25°C (see Table 16). All 24 T_L measurements were reported as being between 950 and 975°C for a spinel primary phase at the lower of the two reported temperatures. The higher temperature of 975°C was used in Reference 22 to represent T_L because this is the highest temperature at which the glasses are known to be amorphous. This type of bounding T_L measurement is inaccurate and cannot accurately be used for model validation although 19 of the 24 T_L values (~80%) did fall within the PCCS liquidus model predictions.

Another study, the PNNL Chemical Variability Study (CVS-I and CVS-II) (see Table 16), was also not usable for liquidus validation as PNNL used a gradient boat method with a 30" long platinum boat. This method is highly inaccurate and is no longer used at PNNL in favor of the isothermal method (ASTM C1720). Due to the inaccuracy of using 30" platinum boats[f] none of this data can be used for model validation. In addition, only thirteen glasses in the CVS-I and CVS-II study met the criteria laid out in Figure 1.

The liquidus data of twenty glasses from an Environmental Management (EM) high waste loaded glass study [118] were available for liquidus validation. The liquidus temperatures were measured by PNNL using ASTM C1720 but the liquidus phase identifications were not reported. Since the DWPF liquidus model is a spinel only model, these data could not be used for validation (Table 16).

Of the remaining 113 liquidus validation glasses generated using ASTM C1720, four did not meet the criteria in Figure 1. Since these glasses were measured using the same ASTM protocol by the same laboratory, these tests [22,124] and the one SRNL melter sample are considered the most accurate liquidus validation data for the PCCS liquidus model. In model data only one of the 105 glass T_L measurements did not fit the model. Therefore, a pooled set of 105+1+109=215 model plus validation glasses of which 30 glasses were not predictable yields a prediction capability of 86%.

[f] Six inch platinum boats were used in the SRNL gradient boat experiments, which were used for model data. This work was performed by Corning Engineering Laboratory Services using ASTM C829 as shown in Table 14.

As with the durability model and the viscosity model, the compositional ranges of the liquidus model overlap for those that validate the PCCS liquidus model and those that do not (Table 17). Note that the validation data cover the zero to 5.00 wt% TiO_2 composition space, while model data does not (Table 17). However, the TiO_2 containing glasses (0 to 5.0) do not fit the current DWPF liquidus model and this is attributed to these glasses being outside the DWPF composition range with 2.0 wt% NiO, 4.0 wt% MnO, 2.4 wt% ZrO_2 and 2.61 wt% CaO (Table 17). This is because the DWPF liquidus model term coefficients were fit to existing data and the glasses that contained TiO_2 only contained up to 1.85 wt% TiO_2. The overlapping oxide ranges are because the PCCS models predict in "property space" and the properties are mathematical functions of the individual oxides.

Table 16. References for Liquidus Model and Validation*

Sample Study	Data Type	Measurement Laboratory	Measurement Method	T_l Measurements			Ref.
				Total	Predictable	NOT Predictable	
Model Data	MODEL	½ SRNL/CELS ½ PNNL	ASTM C829 ASTM C1720	105	104	1	22,23,24
Small Cylindrical (SCM-2) Melter	VALIDATION	SRNL	Melter	1	1	0	23
West Valley (AL,CR,FE,MN, NI,P glasses)	INACCURATE DUE TO BOUNDING METHOD USED	ALFRED UNIVERSITY	Bounding Isothermal	24	19	5	140
PNNL Studies (Chemical Variability Study; CVS-1)	INACCURATE DUE TO 30" GRADIENT BOAT	PNNL	PNNL procedure	13	7	6	98
Hanford High-Iron Tank Waste (SP, MS, US, MISC)	VALIDATION	PNNL	ASTM C1720	113	80	29	22,124
HLW High Waste Loaded Glasses	LIQUIDUS PHASE(S) NOT IDENTIFIED	PNNL	ASTM C1720	20	12	8	118

*Note that the studies shaded in gray could not be used for validation.

Table 17. Composition Regions Covered by the SRNL and PNNL "Spinel Model" Data Sets

Oxide Species (wt%)	Liquidus Model (105 glasses; 55 measured at SRNL and 50 PNNL)[22,23,24]	Melter Validation (Small Cylindrical Melter, SCM-2)[23]	Composite Non-Radioactive and Radioactive Ranges That Fit Model (81 Glasses including SCM-2 Melter)	Composite Non-Radioactive and Radioactive Ranges That Do Not Fit Model (29 Glasses)	DWPF Pour Stream Compositions SB1a-SB7b (1996-2014) (composition from Appendix E; calculated liquidus from 2003 PCCS model)
Temperature (°C)	799-1304	1050	887-1366	893-1273	832-932
Al_2O_3	0.99-14.16	2.5	4.99-14.48	4.00-14.00	3.57-9.83
B_2O_3	4.89-12.65	11.25	4.00-12.00	5.00-10.94	4.27-9.06
BaO	NM	NM	0.00-0.55	0.00-0.55	0.00-0.06
CaO	0.31-2.01	1.06	0.00-5.00	0.01-2.61	0.43-1.39
Cr_2O_3	0.00-0.30	0.077	0.09-1.2	0.00-0.61	0.00-0.16
Cs_2O	NM	NM	0.00	0.00	2.44E-05-1.58E-03
FeO	0.02-6.90	NM	0.00-0.16	0.00-0.17	0.00-2.99
Fe_2O_3	3.43-16.98	20.95	7.31-22.94	6.00-22.99	5.42-12.56
$(\Sigma Fe)_2O_3$	3.45-17.60	20.95	7.42-22.94	6.00-22.99	8.21-12.56
K_2O	0.00-3.89	NM	0.00-4.00	0.00-0.33	0.00-1.80
Li_2O	2.49-6.16	2.81	1.08-6.02	2.22-6.00	3.53-5.55
MgO	0.47-2.65	1.21	0.00-6.02	0.05-1.71	0.22-2.16
MnO	0.74-3.25	4.61	0.00-4.61	0.00-4.00	1.11-2.44
Na_2O	5.99-14.90	10.11	8.35-20.00	9.13-18.86	11.05-14.86
Nd_2O_3	NM	NM	0-0.31	0.00-0.34	0.00
NiO	0.04-3.05	1.53	0.00-3.00	0.00-2.00	0.00-1.38
P_2O_5	NM	NM	0.00-0.80	0.00-0.84	0.00-0.63
SiO_2	41.80-58.23	38.72	30.19-52.99	38.00-60.00	44.77-54.60
SO_4	NM	NM	0-0.40	0.00-0.42	0.00-1.38
TiO_2	0.00-1.85	0.59	0.00-0.39	0.00-5.00	0.00-0.66
U_3O_8	0.00-5.14	NM	0.00-5.53	0.00-5.52	0.00-3.51
ZrO_2	0.00-0.97	0.36	0.00-6.24	0.00-2.37	0.00-0.62

NM = not measured or reported

APPENDIX E. Compositions and Predicted Properties of DWPF Melter Glass from 1994-2014

Table 18. Predicted PCCS Properties Based on Measured Pour Stream Compositions (1994-2014)[17,59,60]

Sample Identification	Durability from THERMO™		Viscosity at 1150°C (Poise)	Resistivity** at 1150°C (Ω•cm)	Liquidus (°C)
	ΔGp (kcal/mole)	Predicted Log NL(B) (g/L)			
WP-14 canister S00009	-7.94	-0.1973	72	4.0	
WP-15 canister S00179	-9.74	-0.0250	52	3.0	
WP-17 canister S00310	-9.75	-0.0245	69	3.8	
SB1a canister S00424	-10.40	-0.0169	57	3.2	919
SB1a canister S00431	-9.34	-0.2099	62	3.4	856
SB1a canister S00471	-10.15	-0.0614	47	2.7	906
SB1a cansiter S00482	-9.52	-0.1758	56	3.1	875
SB1a canister S00834 MFT81*	-9.52	-0.1760	42	2.4	897
SB1b canister S01142 MFT123	-8.82	-0.3025	79	4.3	932
SB2 canister S01913 MFT254	-9.70	-0.1429	40	2.4	916
SB3 canister S02312 MFT319	-9.89	-0.1091	52	3.0	879
SB4 canister S02902 MFT435	-9.75	-0.1350	58	3.3	861
SB5 canister S03317 ARP MFT520	-11.29	0.1452	57	3.2	832
SB6 canister S03465 MFT549	-10.70	0.0378	40	2.4	927
SB6 canister S03472 ARP/MCU MFT551	-11.91	0.2568	46	2.7	892
SB7a canister S03619 MFT 580*	-9.00	-0.2711	68	3.7	930
SB7b canister S04023 MFT 661	-11.09	0.1083	47	2.6	887

*Do not sum to 100±5 wt% oxides [33]

** New resistivity vs. composition model (Equation 10) developed from as measured glass compositions.

Table 19. Measured DWPF Glass Compositions

Oxide (wt%)	Al_2O_3	B_2O_3	BaO	CaO	CdO	Ce_2O_3	Cr_2O_3	CuO	FeO	Fe_2O_3	ΣFe as Fe_2O_3	K_2O	La_2O_3	Li_2O	MgO	MnO
SB1a canister S00424	4.79	8.34	0	0.98	0	0	0.00	0.54	0.00	10.90	10.90	1.80	0.00	3.94	1.81	2.18
SB1a canister S00431	3.57	8.87	0	0.93	0	0	0.00	0.00	0.00	11.50	11.50	0.68	0.00	3.63	1.76	1.44
SB1a canister S00471	4.94	8.87	0	1.26	0	0	0.00	0.48	0.00	12.30	12.30	0.04	0.00	3.74	2.16	1.57
SB1a cansiter S00482	4.57	9.06	0	1.26	0	0	0.00	0.63	0.00	11.40	11.40	0.00	0.00	3.72	2.09	1.44
SB1a canister S00834 MFT81	4.28	8.19	0	1.3	0	0	0.00	0.00	0.00	12.56	12.56	0.00	0.00	3.57	2.10	1.11
SB1b canister S01142 MFT123	5.37	8.18	0.05	1.39	0.03	0	0.08	0.03	0.00	10.50	10.50	0.00	0.02	3.53	2.16	1.76
SB2 canister S01913 MFT254	4.34	4.44	0.05	1.31	0.05	0.06	0.08	0.03	0.00	12.17	12.17	0.00	0.01	5.27	1.16	1.47
SB3 canister S02312 MFT319	4.79	4.44	0.05	1.03	0.14	0.02	0.06	0.01	0.00	10.80	10.80	0.00	0.01	4.96	1.16	2.09
SB4 canister S02902 MFT435	7.78	8.29	0.06	0.72	0.06	0.01	0.06	0.04	1.63	6.40	8.21	0.08	0.01	5.25	0.78	1.62
SB5 canister S03317 ARP MFT520	6.71	5.58	0.04	0.7	0.03	0.06	0.05	0.02	1.77	6.57	8.53	0.04	0.02	5.55	0.51	1.73
SB6 canister S03465 MFT549	9.83	4.91	0.04	0.55	0.01	0.05	0.09	0.03	2.07	6.91	9.21	0.05	0.03	5.04	0.35	2.44
SB6 canister S03472 ARP/MCU MFT551	8.63	4.55	0.06	0.61	0.01	0.04	0.16	0.21	2.99	5.42	8.74	0.09	0.04	4.92	0.33	2.19
SB7a canister S03619 MFT 580	8.59	4.27	0.05	0.46	0.02	0.07	0.07	0.40	0.98	7.28	8.37	0.04	0.04	4.56	0.27	2.01
SB7b canister S04023 MFT 661	7.58	4.72	0.05	0.43	0.02	0.07	0.08	0.19	0.62	7.98	8.67	0.17	0.04	4.83	0.22	1.66
MAX	9.83	9.06	0.06	1.39	0.14	0.07	0.16	0.63	2.99	12.56	12.56	1.80	0.04	5.55	2.16	2.44
MIN	3.57	4.27	0	0.43	0	0	0.00	0.00	0.00	5.42	8.21	0.00	0.00	3.53	0.22	1.11

Table 18. Measured DWPF Glass Compositions (continued)

Oxide (wt%)	MoO_3	Na_2O	NiO	P_2O_5	PbO	SO_4	SiO_2	SrO	ThO_2	TiO_2	U_3O_8	ZnO	ZrO_2	SUM ALKALI	Oxide SUM	$Fe^{2+}/\Sigma Fe$
SB1a canister S00424	0.00	11.20	0.63	0.00	0.00	0.00	52.50	0.00	0.00	0.00	0.00	0.00	0.62	16.94	100.23	0.00
SB1a canister S00431	0.00	11.05	0.00	0.00	0.00	0.00	53.04	0.00	0.00	0.00	0.00	0.00	0.00	15.36	96.47	0.00
SB1a canister S00471	0.00	12.80	0.26	0.00	0.00	0.00	51.30	0.00	0.00	0.00	1.10	0.00	0.06	16.58	100.88	0.00
SB1a cansiter S00482	0.00	11.90	0.00	0.00	0.00	0.00	51.60	0.00	0.00	0.00	1.10	0.00	0.00	15.62	98.77	0.00
SB1a canister S00834 MFT81	0.00	12.08	0.00	0.00	0.00	0.00	48.10	0.00	0.00	0.00	1.03	0.00	0.00	15.65	*94.32*	0.00
SB1b canister S01142 MFT123	0.00	11.50	0.16	0.63	0.01	0.00	52.40	0.00	0.00	0.06	1.06	0.07	0.19	15.03	99.18	0.00
SB2 canister S01913 MFT254	0.03	11.31	0.55	0.48	0.02	0.25	49.31	0.32	0.00	0.06	3.36	0.05	0.08	16.58	96.26	0.00
SB3 canister S02312 MFT319	0.04	11.90	0.55	0.28	0.16	0.39	51.00	0.28	0.00	0.06	3.51	0.01	0.05	16.86	97.80	0.00
SB4 canister S02902 MFT435	0.00	11.50	0.48	0.25	0.01	0.36	50.70	0.01	0.00	0.07	2.23	0.03	0.17	16.83	98.59	0.22
SB5 canister S03317 ARP MFT520	0.01	13.40	0.96	0.21	0.01	0.12	54.60	0.02	0.00	0.20	2.22	0.02	0.11	18.99	101.25	0.23
SB6 canister S03465 MFT549	0.00	13.59	1.11	0.20	0.01	0.24	44.77	0.02	0.68	0.04	2.03	0.03	0.16	18.69	95.31	0.25
SB6 canister S03472 ARP/MCU MFT551	0.01	14.86	1.02	0.09	0.02	0.09	49.10	0.02	1.00	0.35	1.83	0.06	0.12	19.87	98.81	0.38
SB7a canister S03619 MFT 580	0.04	12.45	1.22	0.20	0.08	0.22	47.07	0.03	0.69	0.66	2.43	0.09	0.15	17.05	*94.44*	0.13
SB7b canister S04023 MFT 661	0.01	14.42	1.38	0.15	0.02	0.48	49.42	0.02	0.53	0.25	2.56	0.05	0.09	19.42	98.03	0.08
MAX	0.04	14.86	1.38	0.63	0.16	0.48	54.60	0.32	1.00	0.66	3.51	0.09	0.62	19.87	101.25	0.00
MIN	0.00	11.05	0.00	0.00	0.00	0.00	44.77	0.00	0.00	0.00	0.00	0.00	0.00	15.03	94.32	0.38

Oxide sums in italics do not meet the 100±5 wt% established for a quality analysis of glass. [33]

DISTRIBUTION

S.L. Marra, 773-A
A.P. Fellinger, 773-A
C.C. Herman, 773-A
D.H. McGuire, 773-42A
J.W. Amoroso, 999-W
J.M. Bricker, 704-S
C.L. Crawford, 773-42A
R.E. Edwards, 766-H
T.B. Edwards, 999-W
H.H. Elder, 704-27S
T.L. Fellinger, 766-H
K.M. Fox, 999-W
E.J. Freed, 704-S
C.M. Jantzen, 773-A
F.C. Johnson, 999-W
B.T. Geyer, 704-72S
J.M. Gillam, 766-H
B.A. Hamm, 766-H
E.W. Holtzscheiter, 766-H
J.F. Iaukea, 704-27S
C.J. Martino, 773-42A
J.M. Pareizs, 773-A
J.W. Ray, 704-27S
M.A. Rios-Armstrong, 766-H
H.B. Shah, 766-H
M.E. Stone, 999-W
J.R. Vitali, 704-30S
D.Li, 773-42A
D.L. McClane, 999-W

6.0 References

1 C.M. Jantzen, "**Systems Approach to Nuclear Waste Glass Development,"** J. Non-Cryst Solids ,84 [1-3], 215-225 (1986).

2 C.M. Jantzen, **"Relationship of Glass Composition to Glass Viscosity, Resistivity, Liquidus Temperature, and Durability: First Principles Process-Product Models for Vitrification of Nuclear Waste,"** Proceedings of the 5th International Symposium on Ceramics in Nuclear Waste Management, G.G. Wicks, D.F. Bickford, and R. Bunnell (Eds.), American Ceramic Society, Westerville, OH, 37-51 (1991).

3 C.M. Jantzen and K.G. Brown, **"Statistical Process Control of Glass Manufactured for the Disposal of Nuclear and Other Wastes,"** Am. Ceramic Society Bulletin, 72, 55-59 (May, 1993).

4 **"Preliminary Technical Data Summary for the Defense Waste Processing Facility, Stage 1,"** U.S. DOE Report DPSTD-80-38, E.I. duPont deNemours & Co., Savannah River Plant, Aiken, SC (September, 1980).

5 A. Applewhite-Ramsey, K.Z. Wolf, and M.J. Plodinec, **"EPA Tests of Simulated DWPF Waste Glass,"** Ceramic Transactions, V.29, A.K. Varshneya, D.F. Bickford, and P.P. Bihuniak (Eds.), Amer. Ceramic Society, Westerville, OH, 515-522 (1993).

6 C.M. Jantzen, J.B. Pickett, and I. Joseph, I., **"Toxic Characteristic Leaching Procedure (TCLP) Testing of Waste Glass and K-3 Refractory: Revisited,"** Environmental Issues and Waste Management Technologies in the Ceramic and Nuclear Industries,V, G. T. Chandler (Eds.), Ceramic Transactions, V. 107, 271-280 (2000).

7 M.M. Reigel, **"Literature Review: Assessment of DWPF Melter and Melter Off-gas System Lifetime,"** SRNL-STI-2014-00134 (July 2015).

8 C.M. Jantzen, K.J. Imrich, K.G. Brown, and J.B. Pickett, **"High Chrome Refractory Characterization: Part I. Impact of Melt REDuction/Oxidation (REDOX) on the Corrosion Mechanism in Radioactive Waste Glass Melters,"** International Journal of Applied Glass Science, 6[2], 137-157 (2015).

9 C.M. Jantzen, K.J. Imrich, K.G. Brown, and J.B. Pickett, **"High Chrome Refractory Characterization: Part II. Accumulation of Spinel Corrosion Deposits in Radioactive Waste Glass Melters,"** International Journal of Applied Glass Science, 6[2], 158-171 (2015)

10 C.M. Jantzen and M.J. Plodinec, "Composition and Redox Control of Waste Glasses-Recommendation for Process Control Limit," U.S. DOE Report DPST-86-773 (1986).

11 H.D. Schreiber and A.L. Hockman, **"Redox Chemistry in Candidate Glasses for Nuclear Waste Immobilization,"** J. Am. Ceram. Soc., 70[8], 591-594 (1987).

12 C.M. Jantzen, **"Verification and Standardization of Glass Redox Measurement for DWPF,"** U.S. DOE Report DPST- 89-222 (1989).

13 C.M. Jantzen, J.R. Zamecnik, D.C. Koopman, C.C. Herman, and J.B. Pickett, **"Electron Equivalents Model for Controlling REDuction/OXidation (REDOX) Equilibrium During High Level Waste (HLW) Vitrification,"** U.S. DOE Report WSRC-TR-2003-00126, Rev.0 (May 2003).

14 C.M. Jantzen and F.C. Johnson, **"Impacts of Antifoam Additions and Argon Bubbling on Defense Waste Processing Facility (DWPF) REDuction/OXidation (REDOX),"** SRNL-STI-2011-00652 (April 2012).

15 C.M. Jantzen, F.C. Johnson, M.E. Stone, D.C. Koopman, J.R. Zamecnik, K.G. Brown, J.B. Pickett, and C.C. Herman, **"Melter REDuction/OXidation (REDOX) Control to Optimize Melting and Retain Radionuclides: Part I. High Level Waste Melter REDOX Requirements and Measurement,"** (draft for International Journal of Applied Glass Science).

16 R.L. Postles and K.G. Brown, **"The DWPF Product Composition Control System (PCCS) at Savannah River: Statistical Process Control Algorithm,"** Ceramic Transactions, 23, American Ceramic Society, Westerville, OH, 559-568 (1991).

17 J.W. Amoroso, D.K. Peeler, and T.B. Edwards, **"Elimination of the Characterization of DWPF Pour Stream Sample and the Glass Fabrication and Testing of the DWPF Sludge Batch Qualification Sample,"** U.S. DOE Report SRNL-STI-2012-00157, Savannah River National Laboratory, Aiken, SC (May 2012).

18 C.M. Jantzen, **"Method for Controlling Glass Viscosity (VISCOMP™)."** U.S. Patent #5,102,439, (April, 1992).

19 C.M. Jantzen **"The Impacts of Uranium and Thorium on the Defense Waste Processing Facility (DWPF) Viscosity Model,"** U.S. DOE Report WSRC-TR-2004-00311 (2005).

20 C.M. Jantzen, K.G. Brown, T.B. Edwards, and J.B. Pickett, **"Method of Determining Glass Durability (THERMO™),"** U.S. Patent #5,846,278, (December 1998).

21 C.M. Jantzen, J.B. Pickett, K.G. Brown, T.B. Edwards, and D.C. Beam, **"Process/Product Models for the Defense Waste Processing Facility (DWPF): Part I. Predicting Glass Durability from Composition Using a Thermodynamic Hydration Energy Reaction MOdel (THERMO™)**," U.S. DOE Report WSRC-TR-93-0672, Westinghouse Savannah River Co., Savannah River Technology Center, Aiken, SC, 464p. (1995).

22 K.G. Brown, C.M. Jantzen, and G. Ritzhaupt, **"Relating Liquidus Temperature to Composition for Defense Waste Processing Facility (DWPF) Process Control,"** U.S. DOE Report WSRC-TR-2001-00520, Rev. 0, Westinghouse Savannah River Company, Aiken, SC (October 2001).

23 C.M. Jantzen and Brown, K.G. **"Predicting the Spinel-Nepheline Liquidus for Application to Nuclear Waste Glass Processing: Part I. Primary Phase Analysis, Liquidus Measurement, and Quasicrystalline Approach,"** J. Am. Ceramic Soc., 90 [6], 1866-1879 (2007).

24 C.M. Jantzen and Brown, K.G. **"Predicting the Spinel-Nepheline Liquidus for Application to Nuclear Waste Glass Processing: Part II. Quasicrystalline Freezing Point Depression Model,"** J. Am. Ceramic Soc. 90 [6], 1880-1891 (2007).

25 C.M. Jantzen and J.C. Marra, **"High Level Waste (HLW) Vitrification Experience in the US: Application of Glass Product/Process Control to Other HLW and Hazardous Wastes"** Materials Research Society Symposium Scientific Basis for Nuclear Waste Management XXXI, MRS Symposium Volume 1107, 183-190 (2008).

26 F.C. Johnson, T.B. Edwards, and K.M. Fox, **"The User Guide for the ComPro™ Database,"** SRNL-STI-2009-00093, Revision 1, (2013).

27 F.C. Johnson, T.B. Edwards, and K.M. Fox, **"Data Qualification Report: SRNL Glass Composition – Properties (ComPro™) Database,"** SRNL-STI-2009-00094, Revision 1, (2013).

28 D.K. Peeler, T.B. Edwards, and C.M. Jantzen, **"Task Technical and Quality Assurance Plan for SWPF Integration into the DWPF – Glass Property / Model Impacts,"** U.S. DOE Report SRNL-RP-2014-00348, Savannah River National Laboratory, Aiken, South Carolina (2014).

29 K.M. Fox, et al., **"Refinement of the Nepheline Discriminator: Results of a Phase I Study,**" U.S. DOE Report WSRC-STI-2007-00659, Westinghouse Savannah River Co., Aiken, SC (November 2007).

30 K.M. Fox and T.B. Edwards, **"Refinement of the Nepheline Discriminator: Results of a Phase II Study,**" U.S. DOE Report SRNS-STI-2008-00099, Savannah River Nuclear Solutions, Aiken, SC (October 2008).

31 K.M. Fox and T.B. Edwards, **"Experimental Results of the Nepheline Phase III Study,**" U.S. DOE Report SRNS-STI-2009-00608, Savannah River Nuclear Solutions, Aiken, SC (October 2009).

32 D.K. Peeler and T.B. Edwards, **"Integration of SWPF into DWPF Flowsheet: Gap Analysis and Test Matrix Development,**" U.S. DOE Report SRNL-STI-2014-00578, Savannah River Nuclear Solutions, Aiken, SC (December 2014).

33 C.M. Jantzen, **"Verification of Glass Composition and Strategy for SGM and DWPF Glass Composition Determination,"** U.S. DOE Report DPST-86-708, E.I. DuPont deNemours & Co., Aiken, SC (1986).

34 I. Tovena, T. Advocat, D. Ghaleb, E. Vernaz and F. Larche, **"Thermodynamic and Structural Models Compared with the Initial Dissolution Rates of SON Glass Samples,"** Sci. Basis for Nucl. Waste Mgt., XVII, A. Barkatt and R.A. Van Konynenburg (Eds.), Mat. Res. Soc., Pittsburgh, PA, 595-602 (1994).

35 B.C. Bunker, G.W. Arnold, D.E. Day and P.J. Bray, **"The Effect of Molecular Structure on Borosilicate Glass Leaching,"** J. Non-Cryst. Solids, 87, 226-253 (1986).

36 C.M. Jantzen, K.G. Brown, and J.B. Pickett, **"Durable Glass for Thousands of Years,"** International Journal of Applied Glass Science, 1 [1], 38-62 (2010).

37 M. Tomozawa and S. Sridharan, **"Viscosity Increase of Phase-Separated Borosilicate Glasses,"** J. Am. Ceram. Soc. 75[11], 3103-10 (1992).

38 W. Zheng, M. Lin, J. Cheng, **"Effect of Phase Separation on the Crystallization and Properties of Lithium Aluminosilicate Glass-ceramics,"** Glass Physics and Chemistry, 39 [2], 142-149 (2013).

39 D.F. Bickford and C.M. Jantzen, **"Devitrification of Defense Nuclear Waste Glasses: Role of Melt Insolubles,"** J. Non-Crystalline Solids ,84 [1-3] ,299-307 (1986).

40 D.K. Peeler and T.B. Edwards, **"Impact of REDOX on Glass Durability: The Glass Selection Process,"** U.S. DOE Report WSRC-TR-2004-00135, Rev.0, Westinghouse Savannah River Co., Aiken, SC (March 2004).

41 D.K. Peeler and T.B. Edwards, **"Impact of REDOX on Glass Durability: Experimental Results,"** U.S. DOE Report WSRC-TR-2004-00313, Rev. 0, Westinghouse Savannah River Co., Aiken, SC (June 2004).

42 A.D. Cozzi, T.B. Edwards, D.K. Peeler, and D.R. Best, **"The Impact of REDOX on Durability for Sludge Batch 2,"** U.S. DOE Report WSRC-TR-2003-00246, Rev. 0, Westinghouse Savannah River Co., Aiken, SC (May 2003).

43 Department of Energy, **"Civilian Radioactive Waste Management System Waste Acceptance System Requirements Document, Revision 5,"** U.S. DOE Report DOE/RW-0351 REV. 5 (March 2008).

44 C.M. Jantzen, N.E. Bibler, D.C. Beam, and M.A. Pickett, **"Characterization of the Defense Waste Processing Facility (DWPF) Environmental Assessment (EA) Glass Standard Reference Material,"** U.S. DOE Report WSRC-TR-92-346, Rev. 1, Westinghouse Savannah River Company, Aiken, SC (1993).

45 C.M. Jantzen, N.E. Bibler, D.C. Beam, and M.A. Pickett , "**Development and Characterization of the Defense Waste Processing Facility (DWPF) Environmental Assessment (EA) Glass Standard Reference Material,"** Environmental and Waste Management Issues in the Ceramic Industry, Ceramic Transactions, 39, American Ceramic Society, Westerville, OH, 313-322 (1994).

46 ASTM C1285. **"Standard Test Methods for Determining Chemical Durability of Nuclear, Hazardous, and Mixed Waste Glasses and Multiphase Glass Ceramics: The Product Consistency Test (PCT),**" Annual Book of ASTM Standards, Vol. 12.01, (2014).

47 W.B. White, "**Theory of Corrosion of Glass and Ceramics,"** Corrosion of Glass, Ceramics, and Ceramic Superconductors, D.E. Clark and B.K. Zoitos, Noyes Publications, Park Ridge, NJ, 2-28 (1992).

48 W. Sinkler, T.P. O'Holleran, S.M. Frank, M.K. Richmann, S.G. Johnson, **"Characterization of A Glass-Bonded Ceramic Waste Form Loaded with U and Pu,"** Scientific Basis for Nuclear Waste Management, XXIII, R.W. Smith and D.W. Shoesmith (Eds.), Materials Research Society, Pittsburgh, PA, 423-429 (2000).

49 T. Moschetti, W. Sinkler, T. Disanto, M.H. Hois, A.R. Warren, D. Cummings, S.G. Johnson, K.M. Goff, K.J. Bateman, S.M. Frank, **"Characterization of a Ceramic Waste Form Encapsulating Radioactive Electrorefiner Salt,"** Scientific Basis for Nuclear Waste Management, XXIII, R.W. Smith and D.W. Shoesmith (Eds.), Materials Research Society, Pittsburgh, PA, 577-582 (2000).

50 N.E. Bibler and J.K. Bates, **"Product Consistency Leach Tests of Savannah River Site Radioactive Waste Glasses,"** *Scientific Basis for Nuclear Waste Management*, XIII, Oversby, V. M. and Brown, P. W., eds., Materials Research Society, Pittsburgh, PA, 327–338 (1990).

51 J.K. Bates, D.J. Lam, M.J. Steindler, **"Extended Leach Studies of Actinide-Doped SRL 131 Glass,"** Scientific Basis for Nuclear Waste Management, VI, D.G. Brookins (Ed.), North-Holland, New York, 183-190 (1983).

52 N.E. Bibler and A.R. Jurgensen, **"Leaching Tc-99 from SRP Glass in Simulated Tuff and Salt Groundwaters,"** Scientific Basis for Nuclear Waste Management, XI, M.J. Apted and R.E. Westerman (Eds.), Materials Research Society, Pittsburgh, PA, 585-593 (1988).

53 D.J. Bradley, C.O. Harvey, and R.P. Turcotte, **"Leaching of Actinides and Technetium from Simulated High-Level Waste Glass,"** Pacific Northwest Laboratory Report, PNL-3152, Richland, WA (1979).

54 S. Fillet, J. Nogues, E. Vernaz, and N. Jacquet-Francillon, **"Leaching of Actinides from the French LWR Reference Glass,"** Scientific Basis for Nuclear Waste Management, IX, L.O. Werme, Materials Research Society, Pittsburgh, PA, 211-218 (1985).

55 F. Bazan, J. Rego, and R.D. Aines, **"Leaching of Actinide-doped Nuclear Waste Glass in a Tuff-Dominated System,"** Scientific Basis for Nuclear Waste Management, X, J.K. Bates and W.B. Seefeldt (Eds.), Materials Research Society, Pittsburgh, PA, 447-458 (1987).

56 E.Y. Vernaz and N. Godon, **"Leaching of Actinides from Nuclear Waste Glass: French Experience,"** Scientific Basis for Nuclear Waste Management, XV, C.G. Sombret (Ed.), Materials Research Society, Pittsburgh, PA, 37-48 (1992).

57 W.L. Ebert, S.F. Wolf, and J.K. Bates, **"The Release of Technetium from Defense Waste Processing Facility Glasses,"** Scientific Basis for Nuclear Waste Management, XIX, W.M. Murphy and D.A. Knecht (Ed.), Materials Research Society, Pittsburgh, PA, 221-227 (1996).

58 B.P. McGrail, **"Waste Package Component Interactions with Savannah River Defense Waste Glass in a Low-Magnesium Salt Brine,"** Nuclear Technology, 168-186 (1986).

59 F.C. Johnson and J.M. Pareizs, **"Analysis of Sludge Batch 7a (Macrobatch 8) Pour Stream Samples,**" U.S. DOE Report SRNL-STI-2012-00017, Rev. 0 (May 2012).

60 F.C. Johnson, C.L. Crawford, and J.M. Pareizs, **"Analysis of Sludge Batch 7b (Macrobatch 9) Pour Stream Samples,**" U.S. DOE Report SRNL-STI-2013-00462, Rev. 0 (November 2013).

61 C.M. Jantzen, **"Partial Molar Free Energies of Hydration for XO_2 Species (UO_2, PuO_2, AmO_2, ThO_2, NpO_2) and Potential Non-radioactive Surrogates (HfO_2, ZrO_2, Nd_2O_3) for XO_2 and U_3O_8,"** U.S. DOE Report SRNL-TR-2009-00099, Rev. 0, Savannah River National Laboratory, Aiken, SC (June 2009).

62 C.M. Jantzen, **"Partial Molar Free Energy of Hydration of Niobium Oxide,"** U.S. DOE Report SRNL-TR-2010-00125, Rev. 0, Savannah River National Laboratory, Aiken, SC (October 2010).

63 C.M. Jantzen and K.G. Brown, **"Impact of Phase Separation on Waste Glass Durability,"** Environmental Issues and Waste Management Technologies in the Ceramic and Nuclear Industries, V, G. T. Chandler (Eds.), Ceramic Transactions, V. 107, 289-300 (2000).

64 S.L. Marra, A.L. Applewhite-Ramsey, and C.M. Jantzen. **"DWPF Glass Transition Temperatures-What They Are and Why They Are Important,"** Proceedings of the 5th International Symposium on Ceramics in Nuclear Waste Management, G.G. Wicks, D.F. Bickford, and R. Bunnell (Eds.), American Ceramic Society, Westerville, OH, 465-473 (1991).

65 M.E. Smith, **"Reevaluation of DWPF High Viscosity Constraint: STRC ITS Position,"** SRT-GFM-99-0011 (April 30, 1999).

66 M.J. Plodinec, **"Rheology of Glasses Containing Crystalline Material,"** Advances in Ceramics, V. 20, Nuclear Waste Management II, D.E. Clark, W.B. White, and A.J. Machiels (Eds.), Am. Ceram. Soc., Westerville, OH, 117-124 (1986).

67 G.W. Scherer, **"Editorial Comments on a Paper by Gordon S. Fulcher,"** J. Am. Ceram. Soc, 75 [5], 1060-1062 (1992).

68 ASTM C965. **"Standard Practice for Measuring Viscosity of Glass Above the Softening Point,"** Annual Book of ASTM Standards, Vol. 15.02, (2012).

69 W.B. White and D.G. Minser, **"Raman Spectra and Structure of Natural Glasses,"** J. Non-Cryst. Solids, 67, 45-59 (1984).

70 E.T. Turkdogan, **Physicochemical Properties of Molten Slags and Glasses,** The Metals Society, London (1983).

71 B.O. Mysen, D. Virgo, C.M. Scarfe, and D.J. Cronin, **"Viscosity and Structure of Iron- and Aluminum-Bearing Calcium Silicate Melts at 1 Atm.,"** Am. Mineralogist, 70, 487-498 (1985).

72 B.M.J. Smets and D.M. Krol, **"Group III Ions in Sodium Silicate Glass. Part 1. X-ray Photoelectron Spectroscopy Study,"** Phys. Chem. Glasses, 25 [5], 113-118 (1984).

73 W.L. Konijnendijk, **"Structural Differences Between Borosilicate and Aluminosilicate Glasses Studied by Raman Scattering,"** Glastechn. Ber. 48 [10], 216-218 (1975).

74 T. Furukawa and W.B. White, **"Raman Spectroscopic Investigation of Sodium Borosilicate Glass Structure,"** J. Mat. Sci., 16, 2689-2700 (1981).

75 J. Hlavac, **The Technology of Glass and Ceramics: An Introduction,** Elsevier Scientific Publishing Company, Amsterdam (1983).

76 C.M. Jantzen, and M.J. Plodinec, **"Viscosity and Resistivity of Waste Glasses,"** U.S. DOE Report DPST- 86-372, Rev. 1, E.I. DuPont deNemours & Co, Aiken, SC (1989).

77 D.F. Bickford, A. Applewhite-Ramsey, C.M. Jantzen and K.G. Brown, **"Control of Radioactive Waste Glass Melters: I, Preliminary General Limits at Savannah River,"** J. Am. Ceram. Soc, 73 [10] 2896-2902 (1990).

78 Evgeniĭ ÎUr′evich Tonkov, **High Pressure Phase Transformations: A Handbook**, CRC Press, 732pp. (1982).

79 M.J. Plodinec, **"Long-Term Waste Management Progress Report Small-Scale Electric Melter,"** II. Slag Formation, U.S. DOE Report DPST-78-453, E.I. duPont deNemours & Co., Savannah River Laboratory, Aiken, SC (August, 1978).

80 M.J. Plodinec and J.R. Wiley**, "Viscosity and Electrical Conductivity of Glass Melts as a Function of Waste Composition,"** Proceedings International Symposium on Ceramics in Nuclear Waste Management," CONF-790420, U.S. DOE, Cincinnati, OH, 210-212 (1979).

81 M.K. Andrews and J.R. Harbour, **"Chromium Levels in Feed and Glass for DWPF Startup Melter Campaigns,"** U.S. DOE Report WSRC-TR-95-0368, Westinghouse Savannah River Company, Aiken, SC (September, 1995).

82 F.C. Raszewski and T.B. Edwards, **"Reduction of Constraints for Coupled Operations,"** U.S. DOE Report SRNL-STI-2009-00465, Revision 0, Savannah River National Laboratory, Aiken, SC, (2009).

83 D.K. Peeler and T.B. Edwards, **"SWPF Glass Test Matrix,"** U.S. DOE Memorandum SRNL-L3100-2014-00189, Savannah River National Laboratory, Aiken, SC (August 29, 2014).

84 SAS Institute, Inc., JMP Pro Version 11.2.1, SAS Institute, Inc., Cary, NC (2014).

85 K.G. Brown, R.L. Postles, and T.B. Edwards, **"SME Acceptability Determination for DWPF Process Control,"** WSRC-TR-95-00364, Revision 5 (September 2006).

86 F.C. Raszewski and T.B. Edwards, **"Sludge Batch 7b Glass Variability Study,"** U.S. DOE Report SRNL-STI-2011-00440, Revision 0, Savannah River National Laboratory, Aiken, SC (2011).

87 D.K. Peeler and T.B. Edwards, **"The Sludge Batch 7a Glass Variability Study with Frit 418 and Frit 702,"** U.S. DOE Report SRNL-STI-2011-00063, Savannah River National Laboratory, Aiken, SC (2011).

88 W.K. Kot, I.L. Pegg, D.K. Peeler, and T.B. Edwards, **"Final Report: Sludge Batch 8 Variability Study with Frit 803,"** VSL-13R2580-1 (March 2013).

89 W. Volf, **Glass Science and Technology, 7: Chemical Approach to Glass,** Elsevier Scientific Publishers, New York (1984).

90 J.W. Ray, B.H. Culbertson, S.L. Marra, and M.J. Plodinec, "DWPF Glass Product Control Program," WSRC-IM-91-116-6, Rev. 7 (March 2012).

91 C.M. Jantzen, **"Characterization of Defense Waste Processing Facility (DWPF) Startup Frit,"** U.S. DOE Report WSRC-RP-89-18, Westinghouse Savannah River Co., Aiken, SC (1989).

92 J.V. Crum, R.L. Russell, M.J. Schweiger, D.E. Smith, J.D. Vienna, T.B. Edwards, D.K. Peeler, R. F. Schumacher, and R.J. Workman, **"DWPF Startup Frit Viscosity Measurement Round Robin Results,"** PNNL Report (2001).

93 D.K. Peeler, T.B. Edwards, R.J. Workman, and I.A. Reamer, **"The Impact of Waste Loading on Viscosity in the Frit 418-SB3 System,"** U.S. DOE Report WSRC-TR-2004-00429, Rev. 0, Westinghouse Savannah River Co., Aiken, SC (August 2004).

94 S.L. Marra, and C.M. Jantzen, **"Characterization of Projected DWPF Glasses Heat Treated to Simulate Canister Centerline Cooling,"** U.S. DOE Report WSRC-TR-92-142, Westinghouse Savannah River Co., Savannah River Technology Center, Aiken, SC (May, 1992).

95 C.M. Jantzen, N.E. Bibler, D.C. Beam, C.L. Crawford, C.L., S.L. Marra, A.A. Ramsey, and M.A. Pickett, **"Development and Characterization of the Defense Waste Processing Facility (DWPF) Waste Compliance Plan (WCP) Glasses,"** US DOE Report WSRC-TR-93-181, Westinghouse Savannah River Co., Savannah River Technology Center, Aiken, SC (in preparation 2006). (See also reference 63).

96 T.B. Edwards, J.R. Harbour, R.F. Schumacher, and R.J. Workman, **"Measurement of DWPF Glass Viscosity – Final Report,"** U.S. DOE Report WSRC-RP-99-01053, Westinghouse Savannah River Co., Aiken, SC (November 1999).

97 C.M. Jantzen, **"Sharp-Shurtz (Owens Corning Fiberglass) Data on DWPF Glass,**" DWPT-QA-90-1025 (WSRC-NB-90-394).

98 P. R. Hrma, G. F. Peipel, M. J. Schweiger, D. E. Smith, D. S. Kim, P. E. Redgate, J. D. Vienna, C. A. LoPresti, D. B. Simpson, D. K. Peeler, and M. H. Langowski, **''Property/Composition Relationships for Hanford High-Level Waste Glasses Melting at 1150°C, Vols. 1 and 2''**; U.S. DOE Report PNL-10359, Battelle Memorial Institute, Pacific Northwest Laboratory, Richland, WA, (December 1994).

99 P.D. Soper and D.F. Bickford, **"Physical Properties of Frit 165/Waste Glasses,"** U.S. DOE Report DPST-82-899, E.I. DuPont deNemours & Co., Savannah River Laboratory, Aiken, SC (October 5, 1982).

100 T.B. Edwards, J.R. Harbour, and R.J. Workman, **"Summary of Results for CST Glass Study: Composition and Property Measurements,"** U.S. DOE WSRC-TR-99-00324, Westinghouse Savannah River Co., Aiken, SC (September 1999).

101 T.B. Edwards, J.R. Harbour, and R.J. Workman, **"Composition and Property Measurements for CST Phase 1 Glasses,"** U.S. DOE WSRC-TR-99-00245, Westinghouse Savannah River Co., Aiken, SC (July 1999).

102 T.B. Edwards, J.R. Harbour, and R.J. Workman, **"Composition and Property Measurements for CST Phase 2 Glasses,"** U.S. DOE WSRC-TR-99-00289, Westinghouse Savannah River Co., Aiken, SC (August 1999).

103 T.B. Edwards, J.R. Harbour, and R.J. Workman, **"Composition and Property Measurements for CST Phase 3 Glasses,"** U.S. DOE WSRC-TR-99-00291, Westinghouse Savannah River Co., Aiken, SC (August 1999).

104 T.B. Edwards, J.R. Harbour, and R.J. Workman, **"Composition and Property Measurements for CST Phase 4 Glasses,"** U.S. DOE WSRC-TR-99-00293, Westinghouse Savannah River Co., Aiken, SC (August 1999).

105 T.B. Edwards, J.R. Harbour, and R.J. Workman, **"Summary of Results for PHA Glass Study: Composition and Property Measurements,"** U.S. DOE WSRC-TR-99-00332, Westinghouse Savannah River Co., Aiken, SC (September 1999).

106 T.B. Edwards, J.R. Harbour, and R.J. Workman, **"Composition and Property Measurements for PHA Phase 1 Glasses,"** U.S. DOE WSRC-TR-99-00262, Westinghouse Savannah River Co., Aiken, SC (August 1999).

107 T.B. Edwards, J.R. Harbour, and R.J. Workman, **"Composition and Property Measurements for PHA Phase 1 Glasses,"** U.S. DOE WSRC-TR-99-00290, Westinghouse Savannah River Co., Aiken, SC (August 1999).

108 T.B. Edwards, J.R. Harbour, and R.J. Workman, **"Composition and Property Measurements for PHA Phase 3 Glasses,"** U.S. DOE WSRC-TR-99-00292, Westinghouse Savannah River Co., Aiken, SC (August 1999).

109 T.B. Edwards, J.R. Harbour, and R.J. Workman, **"Composition and Property Measurements for PHA Phase 4 Glasses,"** U.S. DOE WSRC-TR-99-00294, Westinghouse Savannah River Co., Aiken, SC (August 1999).

110 P.B. Macedo, S.M. Finger, A.A. Barkatt, I.L. Pegg, X. Feng, and W.P. Freeborn, **"Durability Testing with West Valley Borosilicate Glass Composition – Phase II,"** DOE/NE/44139-48 (June 1988).

111 D. McPherson, I. Joseph, A. Mathur, C. Capozzi, S. Armstrong, and L.D. Pye, **"The Influence of Waste Variability on the Properties and Phase Stability of West Valley Reference Glass,"** U.S. DOE Report DOE/NE/44139-29 (September 1987).

112 C.M. Jantzen, K.G. Brown, J.B. Pickett, and G.L. Ritzhaupt, **"Crystalline Phase Separation in Phosphate Containing Waste Glasses: Relevance to INEEL HAW,"** WSRC-TR-2000-00339 (September 2000).

113 D.K. Peeler and T.B. Edwards, **"The Impact of Higher Waste Loading on Glass Properties: The Effects of Uranium and Thorium**," U.S. DOE Report WSRC-TR-2003-00386, Rev. 0, Westinghouse Savannah River Co., Aiken, SC (September 2003).

114 C.M. Jantzen and J.B. Pickett, "**M-Area Mixed Waste Glasses: II. Durability and Viscosity Testing of High Aluminum and Uranium Containing Borosilicate Waste Glasses,"** U.S. DOE Report SRNL-STI-2011-00702, Savannah River National Laboratory, Aiken, SC (2015).

115 P. Hrma, J. D. Vienna, M. Mika, J. V. Crum, and G. F. Piepel, **''Liquidus Temperature Data for DWPF Glass,''** U.S. DOE Report PNNL-11790, Pacific Northwest National Laboratory, Richland, WA (1999).

116 K.M. Fox and T.B. Edwards, **"Summary of FY11 Sulfate Retention Studies for Defense Waste Processing Facility Glass,"** U.S. DOE Report SRNL-STI-2012-00152, Savannah River National Laboratory, Aiken, SC (2012).

117 F.C. Raszewski, T.B. Edwards, and D.K. Peeler, **"Matrix 2 Results of the FY07 Enhanced DOE High-Level Waste Melter Throughput Studies at SRNL,"** U.S. DOE Report SRNS-STI-2008-00055, Rev. 0, Savannah River National Laboratory, Aiken, SC (2008).

118 F.C. Raszewski and T.B. Edwards, **"Results of the FY09 Enhanced DOE High-Level Waste Melter Throughput Studies at SRNL,"** U.S. DOE Report, SRNL-STI-2009-00778, Rev. 0, Savannah River National Laboratory, Aiken, SC (2010).

119 K.M. Fox and T.B. Edwards, **"Impacts of Small Column Ion Exchange Streams on DWPF Glass Formulation: KT01, KT02, KT03, and KT04-Series Glass Compositions,"** U.S. DOE Report SRNL-STI-2010-00566, Savannah River National Laboratory, Aiken, SC (2010).

120 K.M. Fox and T.B. Edwards, **"Impacts of Small Column Ion Exchange Streams on DWPF Glass Formulation: KT05 and KT06-Series Glass Compositions,"** U.S. DOE Report SRNL-STI-2010-00687, Savannah River National Laboratory, Aiken, SC (2010).

121 K.M. Fox and T.B. Edwards, "**Impacts of Small Column Ion Exchange Streams on DWPF Glass Formulation: KT07-Series Glass Compositions,"** U.S. DOE Report SRNL-STI-2010-00759, Savannah River National Laboratory, Aiken, SC (2010).

122 K.M. Fox and T.B. Edwards, **"Impacts of Small Column Ion Exchange Streams on DWPF Glass Formulation: KT08, KT09, and KT10-Series Glass Compositions,"** U.S. DOE Report SRNL-STI-2011-00178, Savannah River National Laboratory, Aiken, SC (2011).

123 C.A. Cicero and J.M. Pareizs, **"Viscosity Data from DWPF REDOX Studies,"** U.S. DOE Report SRT-GFM-97-003, Rev. 1, Westinghouse Savannah River Co., Aiken, SC (February 1997).

124 D.S.Kim, P. Hrma, D.E. Smith, and M.J. Schweiger, **"Crystallization in Simulated Glasses from Hanford High-Level Nuclear Waste Composition Range,"** Environmental and Waste Management Issues in the Ceramic Industry, G.B. Mellinger (Ed.), Am. Ceram. Soc., Westerville, OH 179-189 (1990).

125 D.K. Bailey and J.F. Schairer, **"The System Na_2O-Al_2O_3-Fe_2O_3-SiO_2 at 1 Atmosphere, and the Petrogenesis of Alkaline Rocks,"** Journal of Petrology, 7[1], 114-170 (1966).

126 I. M.H. Hager and W. Hinz, **"Beitrag zur Phasentrennunung in Glasern der Systemme Na_2O-SiO_2-B_2O_3 and Na_2O-SiO_2-Al_2O_3,"** Silikatechnik, 18 [11], 360 (1967).

127 J.A. Topping and M.K. Murthy, **"Effect of Small Additions of Al_2O_3 and Ga_2O_3 on the Immiscibility Temperature of Na_2O-SiO_2 Glasses,"** J. Am. Ceram. Soc., 56[5] 270-275 (1973).

128 K.G. Brown and T.B. Edwards, **"Definition of the DWPF Homogeneity Constraint,"** U.S. DOE Report WSRC-TR-95-0060, Westinghouse Savannah River Company, Aiken, SC (1995).

129 T.B. Edwards and K.G. Brown, **"Evaluating the Glasses Batched for the Tank 42 Variability Study,"** Westinghouse Savannah River Company, Aiken, SC, SRT-SCS-98-017, Revision 0 (1998).

130 C.M. Jantzen, C.L. Crawford, J.M. Pareizs, and J.B. Pickett, **"Accelerated Leach Testing of GLASS (ALTGLASS): I. The Database and Definition of High Level Waste (HLW) Glass Hydrogels"** (accepted to International Journal of Applied Glass Science SRNL-STI-2014-00274).

131 C.M. Jantzen, C.L. Crawford, J.M. Pareizs, and J.B. Pickett, **"Accelerated Leach Testing of GLASS (ALTGLASS): II. Mineralization of Hydrogels by Leachate Strong Bases"** (accepted to International Journal of Applied Glass Science SRNL-STI-2014-00381).

132 C.C. Herman, T.B. Edwards, D.M. Marsh, and R.J. Workman, **"Reduction of Constraints: Phase 2 Experimental Assessment for Sludge-Only Processing,"** U.S. DOE Report WSRC-TR-2002-00482, Revision 0, Savannah River National Laboratory, Aiken, SC (2002).

133 C.M. Jantzen, **"Phosphate Additions to Borosilicate Waste Glass Cause Phase Separation,"** U.S. DOE Report DPST-86-389, E.I. DuPont deNemours & Co., Savannah River Laboratory, Aiken, SC (1986).

134 C.M. Jantzen, K.G. Brown, and J.B. Pickett, **"Impact of Phase Separation on Durability in Phosphate Containing Borosilicate Waste Glass for INEEL,"** Environmental Issues and Waste Management Technologies, D.R. Spearing, G.L. Smith, and R.L. Putnam (Eds.), Ceramic Transactions, V. 119, Amer. Ceram. Soc., Westerville, OH, VI, 271-280 (2001).

135 C.M. Jantzen, K.G. Brown, J.B. Pickett, and G.L. Ritzhaupt, **"Crystalline Phase Separation in Phosphate Containing Waste Glasses: Relevance to INEEL HAW,"** WSRC-TR-2000-00339 (September 2000).

136 C.M. Jantzen and D.F. Bickford, **"Leaching of Devitrified Glass Containing Simulated SRP Nuclear Waste,"** Sci. Basis for Nuclear Waste Management, VIII, C.M. Jantzen, J.A. Stone and R.C. Ewing (eds.), Materials Research Society, Pittsburgh, PA 135-146 (1985).

137 H. Li, B. Jones, P. Hrma, J.D. Vienna, **"Compositional Effects on Liquidus Temperature of Hanford Simulated High-Level Waste Glasses Precipitating Nepheline ($NaAlSiO_4$),"** Environmental Issues and Waste Management Technologies in the Ceramic and Nuclear Industries, III, D.K. Peeler and J.C. Marra (Eds.), Am. Ceram. Soc., Westerville, OH, 279-288 (1998).

138 H. Li, P.Hrma, J.D. Vienna, M. Qian, Y. Su, D.E. Smith, **"Effects of Al_2O_3, B_2O_3, Na_2O,and SiO_2 on Nepheline Formation in Borosilicate Glasses: Chemical and Physical Correlations,"** J. Non-Crystalline Solids, 331, 202-216 (2003).

139 T.B. Edwards, D.K. Peeler, and K.M. Fox, **"The Nepheline Discriminator: Reasons for and Details of its Implementation for DWPF's PCCS,"** U.S. DOE Report WSRC-STI -2006-00014, Revision 0, Savannah River National Laboratory, Aiken, SC (2006).

140 I. Joseph, A. Mathur, C. Capozzi, J. Shegal, D. Butts, D.McPherson, L.D. Pye, and L. Eisenstatt. **"Crystallization Behavior of a Fully Simulated West Valley Borosilicate Glass,"** Waste Management 88, pp. 0487-0491 (1988).